Nuclear Physics B (Proc. Suppl.) 3 (1988) 613–638
North-Holland, Amsterdam

Photon Photon Interactions

J. Olsson, DESY

Recent results in $\gamma\gamma$ physics are presented. They include a number of new measurements of the $\gamma\gamma$ widths of members of the $J^{PC} = 0^{-+}$ and 2^{++} SU(3) nonets, a search for 0^{-+} radial excitations, studies of low mass $\pi\pi$ production and new results in the measurements of exclusive η_c and inclusive $D^{*\pm}$ production. Formation of spin=1 resonances in tagged $\gamma\gamma^*$ scattering is described as well as new results in vector meson pair production. Finally new results on the measurement of the photon structure function F_2^γ are reported.

Introduction

In this report space considerations only allow the presentation of the most recent results in $\gamma\gamma$ physics. Even with this restriction there is a large amount of material to cover so brevity has to be exercised. As it happens, most of this summer's experimental results deal with resonance production in $\gamma\gamma$ collisions. All but the last section of this report are therefore devoted to this "soft" domain of $\gamma\gamma$ interactions. Spectroscopy is one of the major fields of interest in $\gamma\gamma$ physics and resonance production results form important contributions to the study of the quark and gluon content of the mesons. The other major field of interest, for many the most important, deals with the possibilities of testing QCD with the $\gamma\gamma$ reactions. Much work has been done in recent years on the measurement of hadron production at high momentum transfers, including the measurement of the photon structure function, from very low Q^2 to the highest available, $\geq 100\ (\mathrm{GeV/c})^2$. The experimental work has been accompanied (and initiated) by the progress in the understanding of the theoretical difficulties of the QCD calculations. In the last section, two new measurements of F_2^γ are reported.

Other important research areas in $\gamma\gamma$ physics include QED-tests to order α^4, the measurement of the total hadronic cross section $\sigma_{tot}(\gamma\gamma \rightarrow hadrons)$ and inclusive hadron production, QCD-tests in the production of meson pairs at large p_t, the production of baryon-pairs and the formation of jets in the reaction $\gamma\gamma \rightarrow q\bar{q}$. The experimental information on these topics has grown considerably in the last years. For recent comprehensive reviews, see the excellent articles in refs.[1,2,3].

The major part of the $\gamma\gamma$ physics results comes from the detectors at the high luminosity e^+e^- storage rings PEP, PETRA and DORIS. The PETRA experiments doubled their statistics in the last year of machine operation, thereby reaching integrated luminosities comparable to the PEP experiments, and some results are now available from these high statistics data. Remarkably, the PLUTO experiment is still delivering important results, 5 years after closing down. Judging from this, we shall see new results coming forth from the other PETRA experiments still in the early 1990s!

Pseudoscalars and Tensors

No less than 12 new measurements of the $\gamma\gamma$ widths of the neutral members of the 0^{-+} and 2^{++} nonets are presented this year; either completely new measurements or updates of earlier, preliminary measurements. Only the $f_2(1270)$ meson is not represented. The new results are summarized in Table 1. It is not possible to present all this new data here in any detail or even to show all the relevant histograms, but some brief descriptions will be given.

The measurements by the Crystal Ball collaboration [4] of the radiative widths of π°, η and η' using data on $\gamma\gamma$ elastic scattering are now given with final values. The data are shown in Fig. 1. This is the first measurement of $\Gamma_{\pi^\circ\gamma\gamma}$ to use $\gamma\gamma$ collisions in an e^+e^- storage ring, a method originally suggested by Low [5]. It is in good agreement both with the recent high precision life time measurement,

$7.25 \pm 0.18 \pm 0.11$ eV [6] and with the older Primakoff scattering measurements, 8.0 ± 0.4 eV [7]. As is well known, this is in striking contrast to the situation with the η width, where the e^+e^- measurements disagree with both of the Primakoff scattering measurements [8]. For a full discussion on this disagreement, see refs.[9,10]. The precision of the new Crystal Ball measurement is even higher than that of the previous measurement by the JADE collaboration, $0.53 \pm 0.04 \pm 0.04$ keV [11]. All e^+e^- measurements of $\Gamma_{\eta\gamma\gamma}$ are in excellent agreement.

Meson	Decay Mode	$\Gamma_{\gamma\gamma} \pm \sigma(stat.) \pm \sigma(syst.)$ (keV)	Experiment	Ref.
π°	$\gamma\gamma$	$0.0077 \pm .0005 \pm .0005$	Crystal Ball	[4]
η	$\gamma\gamma$	$0.514 \pm .017 \pm .035$	Crystal Ball	[4]
η'	$\gamma\gamma$	$5.6 \pm .6 \pm .6$	Crystal Ball	[4]
	$\eta\pi^\circ\pi^\circ, \eta \to \gamma\gamma$	$4.6 \pm .4 \pm .6$	Crystal Ball	[17]
	$\eta\pi^+\pi^-, \eta \to \gamma\gamma$	$4.7 \pm .6 \pm .9$	Mark II	[15]
	$\eta\pi^+\pi^-, \eta \to \gamma\gamma$	$3.80 \pm .13 \pm .50$	JADE (prel.)	[16]
	$\gamma\rho^\circ$	$3.76 \pm .13 \pm .47$	ARGUS	[13]
	$\gamma\rho^\circ$	$4.6 \pm 1.1 \pm .9$	MD-1 (prel.)	[18]
$a_2(1320)$	$\rho^\pm\pi^\mp$	$0.97 \pm .10 \pm .22$	TPC/2γ (prel.)	[19]
	$\rho^\pm\pi^\mp$	$1.05 \pm .24 \pm .23$	MD-1 (prel.)	[18]
$f_2'(1525)$	$K_S^\circ\overline{K_S^\circ}$	$0.11\ ^{+.03}_{-.02} \pm .02$	CELLO (prel.)	[22]
	$K_S^\circ\overline{K_S^\circ}$	$0.10\ ^{+.04}_{-.03}\ ^{+.03}_{-.02}$	PLUTO	[23]

Table 1: New measurements of the $\gamma\gamma$ widths of pseudoscalar and tensor mesons. In case of $f_2'(1525)$, the measured values represent $\Gamma_{f_2'\gamma\gamma} \cdot BR(f_2' \to K\overline{K})$.

Weighted Means of $\Gamma_{\gamma\gamma}$ (keV)	
$\Gamma_{\pi^\circ\gamma\gamma} = 0.00729 \pm 0.00019$	$\Gamma_{a_2\gamma\gamma} = 0.96 \pm 0.11$
$\Gamma_{\eta\gamma\gamma} = 0.524 \pm 0.031$	$\Gamma_{f_2'\gamma\gamma} = 0.10 \pm 0.02$
$\Gamma_{\eta'\gamma\gamma} = 4.25 \pm 0.19$	$\Gamma_{f_2\gamma\gamma} = 2.84 \pm 0.16$

Table 2: Weighted means of $\gamma\gamma$ widths of pseudoscalar and tensor mesons. Statistical and systematic errors have been added in quadrature. Primakoff scattering measurements are not included. In case of $f_2'(1525)$, it is assumed that $BR(f_2' \to K\overline{K}) = 100\%$. For a list of $\Gamma_{\gamma\gamma}$ measurements not quoted in Table 1, see ref.[12]. No effort has been made to avoid double-counting of common errors, e.g. errors on branching ratios.

Six new measurements of $\Gamma_{\eta'\gamma\gamma}$ are listed in table 1, now making this quantity the most measured one, from altogether 17 different experiments. Of the new ones, only two are obtained using the decay mode $\eta' \to \gamma\rho^\circ$. This is otherwise the decay mode most used, readily within reach of the triggering possibilities of most e^+e^- detectors. Since it is a magnetic dipole transition, followed by the ρ decay, the Monte Carlo simulation has to use a fairly complicated matrix element [3]. It is

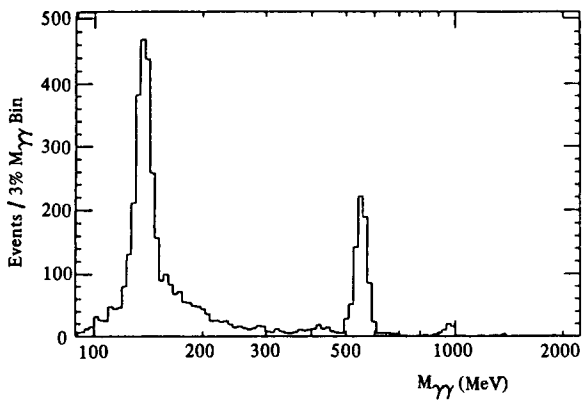

Figure 1: Inv. $\gamma\gamma$ mass in the reaction $\gamma\gamma \rightarrow \gamma\gamma$. Crystal Ball data from 46 pb^{-1}; the π^0 peak contains 1200 events. For the $\Gamma_{\eta\gamma\gamma}$ and $\Gamma_{\eta'\gamma\gamma}$ measurements 114 pb^{-1} were used. Note the mass scale.

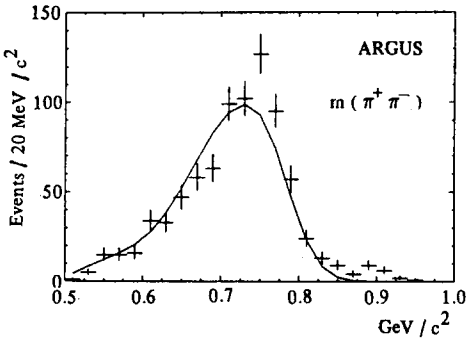

Figure 2: Inv. $\pi^+\pi^-$ mass in the reaction $e^+e^- \rightarrow e^+e^-\eta'$, $\eta' \rightarrow \pi^+\pi^-\gamma$. ARGUS data from 107 pb^{-1}; The ρ peak contains 870 events. The curve shows the MC simulation.

interesting to note that this matrix element in fact does not describe the data exactly. This is clearly demonstrated in the high statistics data of the ARGUS collaboration[13], shown in Fig. 2. As seen, the $\pi^+\pi^-$ mass spectrum is harder in the data than the Monte Carlo simulation predicts (with a corresponding systematically weaker photon energy spectrum in the real data). The same systematic effect is seen in other experiments that have used the dipole transition matrix element in their analyses [14]. The reason for this deviation is not clear; the dipole transition is without dispute, but a different parametrisation of the ρ Breit-Wigner form could perhaps be considered.

To avoid these difficulties, several experiments have used other decay modes for measuring $\Gamma_{\eta'\gamma\gamma}$, namely $\eta' \rightarrow \gamma\gamma$ and $\eta' \rightarrow \eta\pi\pi$. The $\eta\pi^+\pi^-$ decay involves pions of lower energy than in the ρ decay, and these events are correspondingly more difficult to trigger on. The Mark II [15] measurement is based on data taken at PEP with reduced magnetic field (short circuit in coil), which enabled the triggering on low momentum pions. The data are shown in Fig. 3. In the JADE measurement [16], the photons from the η decay were used in the trigger. Both fully reconstructed 2-prong 2-γ events and incompletely reconstructed 1-prong, 2-γ events are used in the analysis, since the low Q-value of this η' decay leads to a clear resonant structure in the $\eta\pi^\pm$ mass distribution. The data are shown in Figs. 4a and 4b. The combination of both 2-prong and 1-prong samples gives a handle on the uncertainties in the Monte Carlo simulation of low energy pions and thereby helps in reducing the systematic error, apart from adding to the fair statistics.

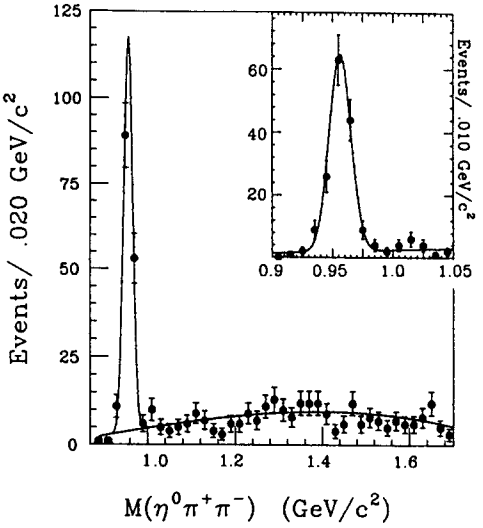

Figure 3: Inv. $\eta\pi^+\pi^-$ mass in the reaction $e^+e^- \rightarrow e^+e^-\eta\pi^+\pi^-$. Data from Mark II coll. corresponding to 220 pb^{-1}. The η' peak contains 143±12 events.

The completely neutral decay mode, $\eta' \rightarrow \eta\pi^0\pi^0$, with 6 photons in the final state, is so far only accessible to the Crystal Ball experiment [17]. Their data are shown in Fig. 11a.

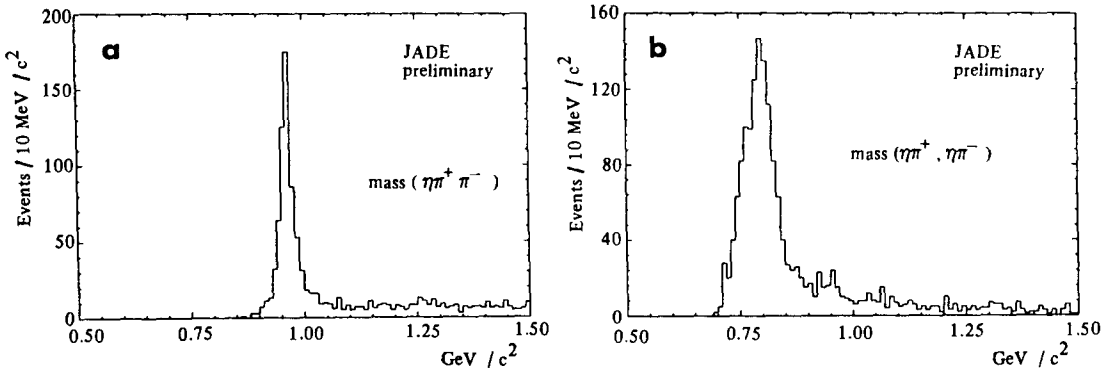

Figure 4: **a)** Inv. $\eta\pi^+\pi^-$ mass and **b)** Invariant $\eta\pi^\pm$ mass from the reaction $e^+e^- \to e^+e^-\ \eta\pi^+\pi^-$. Data from JADE coll. with 170 pb^{-1}. The η' peaks contain 500 and 1100 events, respectively.

The $\pi^+\pi^-\gamma$ final state is used by the MD-1 collaboration [18] for determining both $\Gamma_{\eta'\gamma\gamma}$ and $\Gamma_{a_2\gamma\gamma}$; in the latter case, the $\rho^\pm\pi^\mp$ final state is not fully reconstructed. The preliminary data are shown in Fig. 5. In this experiment a transverse magnetic field of 1.2 Tesla is applied and therefore the outgoing, scattered electrons can be detected (0°–tagging). At least 1 measured electron is used in the reconstruction of the events.

Also the TPC/2γ collaboration[19] have measured $\Gamma_{a_2\gamma\gamma}$ (Fig. 6). They have enough statistics to undertake the study of the angular correlations in the decay $a_2(1320) \to \rho^\pm\pi^\mp, \rho^\pm \to \pi^\pm\pi^\circ$, and conclude that the formation of $a_2(1320)$ proceeds dominantly (85 ± 10 %) in a helicity 2 state. This is in agreement with earlier studies [20] and with theoretical expectations for the tensor mesons [21].

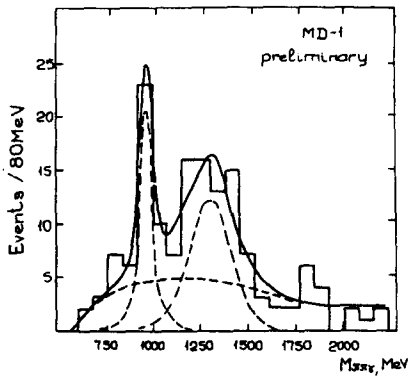

Figure 5: Inv. $\pi^+\pi^-\gamma$ mass in the reaction $e^+e^- \to e^+e^-\ \pi^+\pi^-\gamma(\gamma)$. Data from MD-1 coll. at VEPP-4, with 20 pb^{-1}. The curves show the polynomial background and the contribution from a_2 and η'. Cuts optimal for determining $\Gamma_{a_2\gamma\gamma}$.

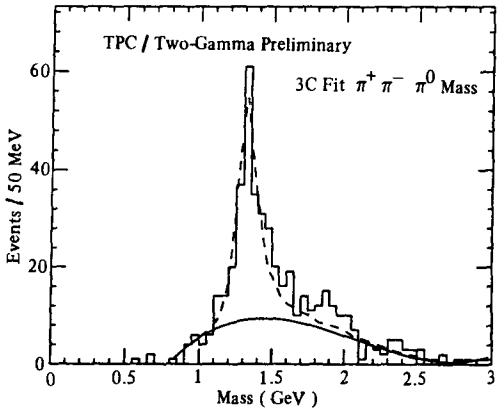

Figure 6: $\pi^+\pi^-\pi^\circ$ inv. mass in the reaction $e^+e^- \to e^+e^-\pi^+\pi^-\pi^\circ$. TPC/2$\gamma$ data corresponding to 143 pb^{-1}. The curves show the polynomial background and the a_2 contribution.

There are two new measurements of $\Gamma_{f_2'\gamma\gamma}$, or rather the product $\Gamma_{f_2'\gamma\gamma} \cdot$ BR($f_2'(1525) \to K\overline{K}$), by the CELLO and PLUTO collaborations. Both use the decay $f_2'(1525) \to K_S^\circ\overline{K_S^\circ}$, $K_S^\circ \to \pi^+\pi^-$. The preliminary CELLO data [22] are shown in Fig. 7. In the PLUTO analysis [23] use is made of the forward spectrometers to extend the sensitive range in order to measure, for the first time, the helicity structure of the f_2' formation. The angular distributions in $\cos\theta^*$, θ^* being the decay angle in

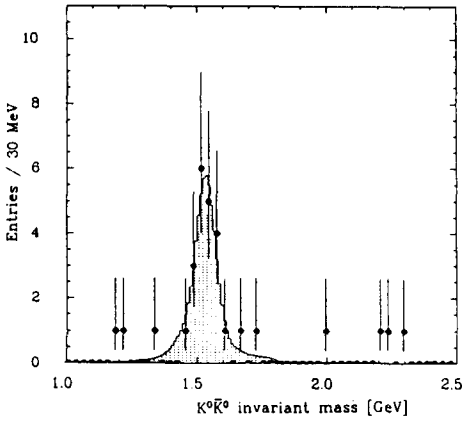

Figure 7: Inv. $K^0_S\overline{K^0_S}$ mass in the reaction $e^+e^- \to e^+e^-\ \pi^+\pi^-\pi^+\pi^-$. Prel. CELLO data corresponding to 90 pb^{-1}. There are 15 $f_2'(1525)$ events.

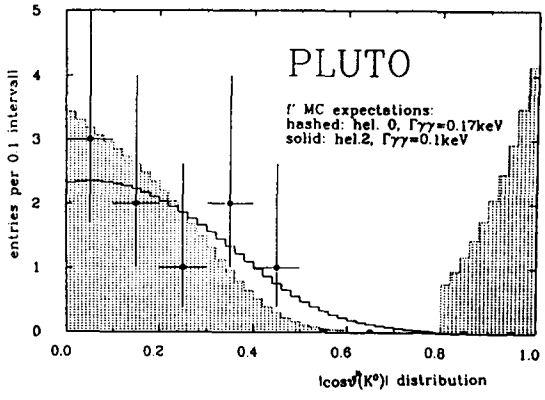

Figure 8: $|\cos\theta^*|$ for events with $m(K^0_S\overline{K^0_S})$ in band 1.35–1.7 GeV/c^2. θ^* is the decay angle in the C.M. system of f_2'. Solid and shaded histograms: MC expectations for helicity 2 and 0. PLUTO data, 45 pb^{-1}and 9 f_2' events.

the C.M. system of f_2', is widely different for helicity 0 and helicity 2 formation (Fig. 8). The result, $\Gamma^{(hel.0)}_{f_2'\gamma\gamma}/\Gamma_{f_2'\gamma\gamma} < 0.60$ at 95 % c.l., is, despite the low statistics, an important support for the expected helicity 2 dominance. Moreover, their measured result for $\Gamma_{f_2'\gamma\gamma}$ (Table 1) is independent of helicity structure assumptions. Previous measurements had to rely on the assumed helicity 2 dominance.

The weighted means of the various $\gamma\gamma$ widths of the pseudoscalars and tensors are listed in Table 2. These couplings give information about the charge content of the mesons and can be used to test ideas about their quark structure. With current algebra and SU(3), one can derive the relations [24,25]

$$\Gamma_{\eta\gamma\gamma} = \frac{1}{3}\left(\frac{m_\eta}{m_{\pi^\circ}}\right)^3 \Gamma_{\pi^\circ\gamma\gamma}\left(\sqrt{8}\,\frac{f_\pi}{f_1}\sin\theta - \frac{f_\pi}{f_8}\cos\theta\right)^2$$

$$\Gamma_{\eta'\gamma\gamma} = \frac{1}{3}\left(\frac{m_{\eta'}}{m_{\pi^\circ}}\right)^3 \Gamma_{\pi^\circ\gamma\gamma}\left(\frac{f_\pi}{f_8}\sin\theta + \sqrt{8}\,\frac{f_\pi}{f_1}\cos\theta\right)^2,$$

where θ is the SU(3) singlet–octet mixing angle and f_1, f_8, f_π are PCAC decay constants. In potential models, the f_i are spatial wave functions evaluated at the origin. SU(3) symmetry implies $f_8 = f_\pi$. The same relations are normally assumed to hold for the tensor mesons, with the replacements $\eta \to f_2'$, $\eta' \to f_2$ and $\pi^\circ \to a_2$, although the power of the mass-ratio factors is less certain in this case[3]. For the tensors, the f_i are derivatives of wave functions (P-wave). Setting $r = f_\pi/f_1$ and assuming SU(3) symmetry, one finds

$$r_P = 0.94 \pm 0.02 \qquad r_T = 1.06 \pm 0.03$$
$$\theta_P = -18.4^\circ \pm 1.1^\circ \qquad \theta_T = 26.6^\circ \pm 1.1^\circ.$$

The large negative mixing angle for the pseudoscalars is well known; it differs from both the quadratic ($\theta_P = -10^\circ$) and the linear ($\theta_P = -23^\circ$) mass formula values. In ref.[26] it is shown that with a 1st order correction in chiral perturbation theory, SU(3) is broken for the pseudoscalars: $f_8 \approx 1.25 f_\pi$. Using this in the above formula, one obtains $r_P = 0.97 \pm 0.02$ and $\theta_P = -22.7^\circ \pm 1.1^\circ$ as well as the quadratic mass formula value $\theta_P = -19.5^\circ$ [26]. Thus a consistent picture can be obtained for the large negative mixing angle of the pseudoscalars. For an extensive discussion, see ref.[27]. For the tensors, r_T and θ_T are in good agreement with nonet symmetry ($r_T = 1$) and the quadratic mass formula value $\theta_T = 28^\circ$, close to the ideal mixing value of 35.26°.

The deviations from ideal mixing in the pseudoscalar nonet have been subject of much theoretical work, in particular concerning the possibility that this nonet is mixed with additional gluonic matter. The approach of Rosner [28] provides a nice graphical illustration, shown in Fig. 9. Here the plane $|X\rangle = \frac{1}{\sqrt{2}}|u\bar{u} + d\bar{d}\rangle, |Y\rangle = |s\bar{s}\rangle$ in $u\bar{u}, d\bar{d}, s\bar{s}$ space is displayed. Both isoscalars lie in this plane, $|\eta\rangle = x_\eta|X\rangle + y_\eta|Y\rangle$ and $|\eta'\rangle = x_{\eta'}|X\rangle + y_{\eta'}|Y\rangle$. Since also other radiative decays of η and η' can be expressed in this formalism (see ref.[28]), constraints are obtained on the coefficients $x_{\eta,\eta'}$ and $y_{\eta,\eta'}$. These are shown in Fig. 9. Several comments can be made:

The relatively broad limits on y_η (from $\phi \to \gamma\eta$) and x_η (from $\rho \to \gamma\eta$), together with the narrow band from $\eta \to \gamma\gamma$, provide a solution for x_η and y_η close to and on the boundary $x^2 + y^2 = 1$ and with small errors. Since with additional gluonium matter one would have $|\eta\rangle = x_\eta|X\rangle + y_\eta|Y\rangle + g_\eta|G\rangle$, with $x_\eta^2 + y_\eta^2 + g_\eta^2 = 1$, it is clear that η is a pure $q\bar{q}$ state, with very little room for additional gluonium.

In the case of η', the only $y_{\eta'}$ information comes from the narrow band $\eta' \to \gamma\gamma$; it cuts the band limiting $x_{\eta'}$ (from $\eta' \to \gamma\rho$) and from the common area one concludes that $y_{\eta'}$ could well have a quite small value, allowing for a substantial admixture of gluonium matter $|G\rangle$. Unfortunately, the radiative decay $\phi \to \gamma\eta'$, which would provide further information on $y_{\eta'}$, has not yet been measured. A recent upper limit from VEPP-2M [29], $BR(\phi \to \gamma\eta') < 4.1 \cdot 10^{-4}$ at 90 % c.l., is far outside of Fig. 9.

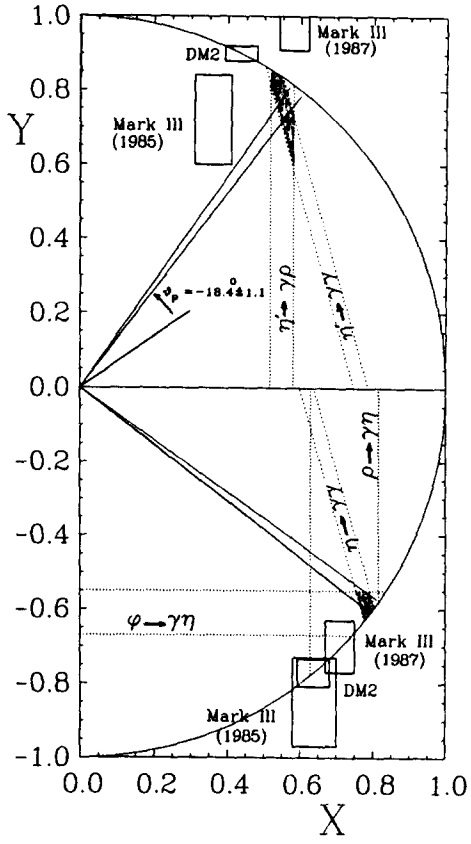

Figure 9: Rosner plot for the pseudoscalars.

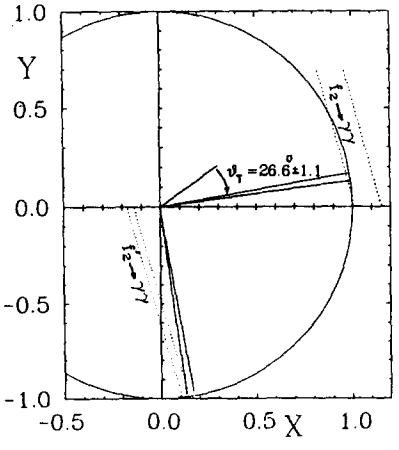

Figure 10: Rosner plot for the tensors.

Additional information comes from measurements of the decays J/ψ →pseudoscalar + vector, i.e. the decays J/$\psi \to \rho\eta, \rho\eta', \omega\eta, \omega\eta', \phi\eta$ and $\phi\eta'$. These decays can also be analysed in terms of the formalism above. The result of an early analysis by the Mark III collaboration [30] is displayed in Fig. 9. This result, which indicated a large non-$q\bar{q}$ component in η', caused some concern, since it disagrees with the data from $\eta' \to \gamma\gamma$ and $\eta' \to \gamma\rho^\circ$. Recently the analysis has been remade [31], also by the DM2 collaboration[32]. The additional inclusion of doubly disconnected diagrams (DOZI), with the pseudoscalar connected only by gluon lines to the J/ψ and the vector, turns out to be important. The new solutions are shown in Fig. 9 and one can conclude that also in the case of η', there is no need for an additional gluonium component. For further discussion, see also ref.[33].

In the $|X\rangle, |Y\rangle$ plot for the tensor mesons f_2 and f_2', Fig. 10, the $\gamma\gamma$ decays are the only ones to provide information on the values of $x_{f_2,f_2'}$ and $y_{f_2,f_2'}$. The

plot illustrates the almost ideal mixing in the tensor nonet, with the $f_2 \rightarrow \gamma\gamma$ band just touching the border $x^2 + y^2 = 1$; the f_2 is a pure $u\bar{u}$, $d\bar{d}$ state with little $s\bar{s}$. The f_2', although compatible with an almost pure $s\bar{s}$ state, could well be mixed with additional gluonium.

To finish this section, it is worthwhile to make two remarks: **(a)** The weighted means of the $\gamma\gamma$ widths of the pseudoscalars have now reached a high precision, e.g. $\Gamma_{\eta'\gamma\gamma}$ is known to ~ 4 % precision, to be compared with the first measurement in 1979 by D.Binnie et al., 5.4±2.1 keV [34]. However, this precision does not propagate into the total width of η' ($\Gamma_{\eta'} = 227 \pm 22$ keV) and the other partial widths, since $BR(\eta' \rightarrow \gamma\gamma)$ is only known with ~ 10 % precision[35]. For further work of the kind described above, $BR(\eta' \rightarrow \gamma\gamma)$ is a key number and ought to be given more experimental attention. **(b)** It should be noted that the measurement of $\Gamma_{\eta'\gamma\gamma}$ by Binnie et al. (which is a total width measurement, $\Gamma_{\eta'\gamma\gamma}$ is obtained via $BR(\eta' \rightarrow \gamma\gamma)\cdot\Gamma_{\eta'}$), and the e^+e^- measurements of $(2J+1)\cdot\Gamma_{\eta'\gamma\gamma} = 4.2\pm0.2$ keV, together determine the spin J of η' to be $J = 0$, without doubt [36]. This relation is important and ought to be included in the PDG summary.

Radial excitations of Pseudoscalar mesons

Much experimental and theoretical work has gone into the understanding of the radial excitations of the SU(3) nonets, especially the pseudoscalar one [37,38,39,40,41]. The pseudoscalar 2S states are expected to have masses between 1 and 2 GeV/c^2 and the strongest candidates for the neutral members are $\eta(1275), \eta(1400)$ and $\pi(1300)$. For their present experimental status, see ref.[9,42] The Crystal Ball group have investigated the possible production of these states in $\gamma\gamma$ collisions, both in the final state $\eta\pi^\circ\pi^\circ$[17], where the two former candidates could be expected to appear [38], and in the final state $\pi^\circ\pi^\circ\pi^\circ$[43], with $\pi(1300)$ decaying to $\pi(\pi\pi)_{s-wave}$. Both of these final states consist of 6 photons; the Crystal Ball results are shown in Figs. 11 and 12.

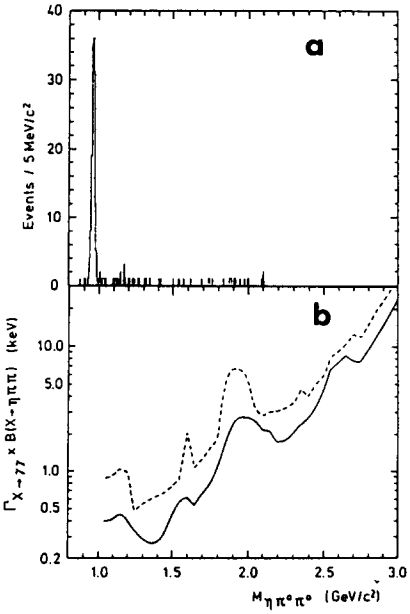

Figure 11: **a)** Inv. $\eta\pi^\circ\pi^\circ$ mass in the reaction $e^+e^- \rightarrow e^+e^-\ \eta\pi^\circ\pi^\circ$. Data from Crystal Ball coll., with 131 pb^{-1}; the η' peak contains 185±14 events. **b)** 90 % c.l. upper limits for $\Gamma_{X\gamma\gamma}\cdot BR(X\rightarrow \eta\pi\pi)$, with X having spin=0. Solid and dashed curves: $\Gamma_X = 50$ and 200 MeV.

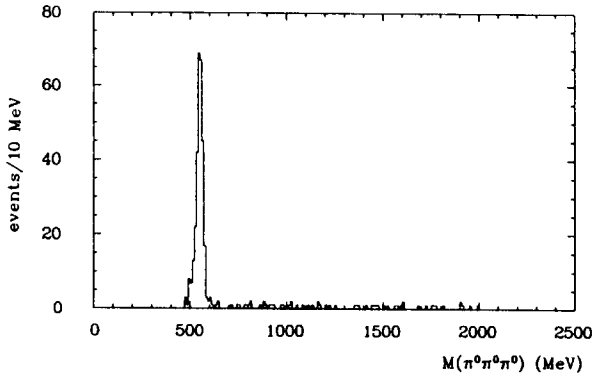

Figure 12: Inv. $\pi^\circ\pi^\circ\pi^\circ$ mass in the reaction $e^+e^- \rightarrow e^+e^-\pi^\circ\pi^\circ\pi^\circ$. Crystal Ball data with 219 pb^{-1}.

As seen, the only resonant contributions in these spectra are the impressive η' and η peaks. In the $\eta\pi^\circ\pi^\circ$ case, the data have been used to calculate limits for the $\gamma\gamma$ production of narrow states up to 3 GeV/c^2; they are shown in Fig. 11b. Also $\Gamma_{\eta'\gamma\gamma}$ is measured, see Table 1. The $\pi^\circ\pi^\circ\pi^\circ$ spectrum has not yet been quantitatively evaluated. The limits for $\Gamma_{X\gamma\gamma}\cdot BR(X\rightarrow \eta\pi\pi)$ are as low as 0.3 keV. Several keV for the $\gamma\gamma$ widths of excited η and η' have been predicted[39,40]. Unless $BR(\eta\pi\pi)$ is small, these models are excluded for $\eta(1275)$. In a contributed paper [41] a width compatible with the limit is predicted, although the model used predicts too high a value for $\Gamma_{\eta\gamma\gamma}$.

The low mass part of the $\pi\pi$ spectrum

The final analysis of the 2-prong data obtained with the DM1 and DM2 detectors is now presented [44]. The two data sets have been added. In the $\pi^+\pi^-$ final state, shown in Fig. 13, an excess of events is seen above the Born term prediction at lowest masses. The observed no. of events is 52±11, the expectation is 29±2. The statistical significance of this is low, but the spectrum gains interest when comparing with the excess at lowest masses ($\sim$ 400 MeV/c^2) in the $\pi^+\pi^-$ spectrum, observed by the PLUTO collaboration [45] and shown in Fig. 14. The possibility of a resonant contribution in this mass region is excluded [1] by the new high statistics data from the Crystal Ball collaboration[43] on $\gamma\gamma \to \pi^0\pi^0$, shown in Fig. 15. Interestingly, the cross section $\sigma(\gamma\gamma \to \pi^0\pi^0)$ extends right down to threshold with a finite value. Whether this is connected to the production of a very broad, low mass f_0 or something else remains to be seen. The complex question of low mass $\pi\pi$ production in $\gamma\gamma$ collisions is extensively discussed in several recent articles[47,48].

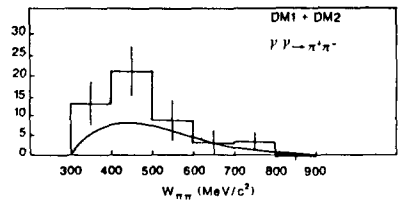

Figure 13: Inv. $\pi^+\pi^-$ mass in the reaction $e^+e^- \to e^+e^-\pi^+\pi^-$. DM1 and DM2 data added, $\sim$ 800 nb^{-1}. The curve shows the Born MC expectation.

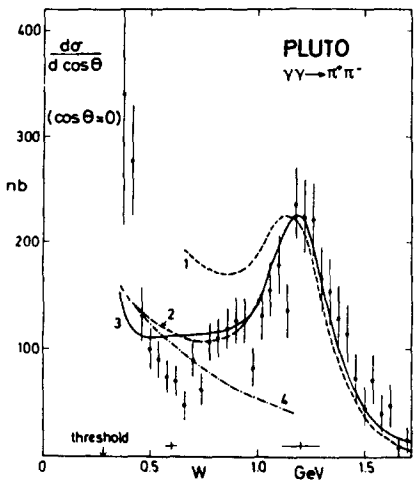

Figure 14: Inv. $\pi^+\pi^-$ mass in the reaction $e^+e^- \to e^+e^-\pi^+\pi^-$. PLUTO data from 13 pb^{-1} and with $|\cos\theta^*| < 0.20$. The curve labeled 4 shows Born term expectation.

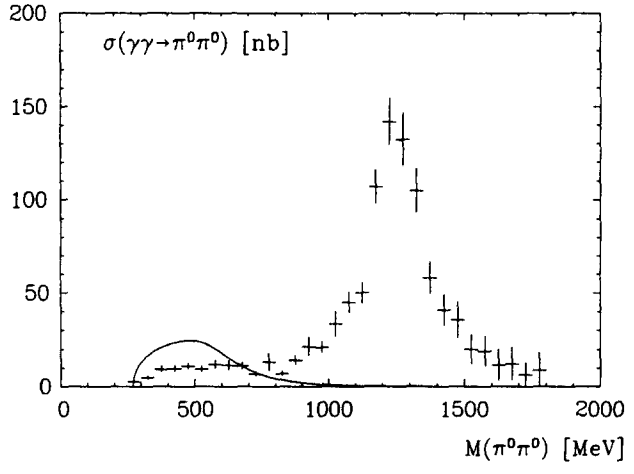

Figure 15: Inv. $\pi^0\pi^0$ mass in the reaction $e^+e^- \to e^+e^-\pi^0\pi^0$. Prel. Crystal Ball data from 92 pb^{-1}. The curve shows the MC expectation from $\gamma\gamma \to f_0(600), f_0 \to \pi^0\pi^0$, with $\Gamma_{f_0} =$ 400 MeV and $\Gamma_{f_0\gamma\gamma}$ =1 keV. $|\cos\theta^*| < 0.80$ for data and MC simulation. For the data, $\sigma(\gamma\gamma \to \pi^0\pi^0)$ is independent of spin and helicity assumptions.

Measurement of the $\gamma\gamma$ width of $\eta_c(2981)$

The interest in measuring $\Gamma_{\eta_c\gamma\gamma}$ comes e.g. from the relation [49]

$$\frac{\Gamma(\eta_c \to hadrons)}{\Gamma(\eta_c \to \gamma\gamma)} = \frac{2}{9}\frac{[\alpha_s^{\overline{MS}}(m_{\eta_c}^2)]^2}{\alpha^2}\frac{1}{\epsilon_c^4}\left\{1 + \frac{14.00\alpha_s^{\overline{MS}}(m_{\eta_c}^2)}{\pi} + \mathcal{O}\left(\left(\frac{\alpha_s^{\overline{MS}}(m_{\eta_c}^2)}{\pi}\right)^2\right)\right\}$$

which allows to measure α_s, knowing the total hadronic width of η_c. It has been pointed out [50] that this and similar relations for other charmonium (χ_0^{++}, χ_2^{++}) and bottomonium states provide very

[1] Although no quantitative limit is given yet for the Crystal Ball data, the value (10±6 keV) earlier quoted for a $\gamma\gamma$ width by the DM1 group[46] is clearly excluded.

clean tests of perturbative QCD, if ratios can be precisely measured. However, from the relation

$$\sigma(e^+e^- \rightarrow e^+e^-\eta_c)\ (nb) \ \sim \ 0.25\frac{\Gamma_{\eta_c\gamma\gamma}\ (keV)}{m^3_{\eta_c}\ (GeV)}$$

and with BR($\eta_c \rightarrow$X) $\sim$ few % (including secondary branching ratios of the exclusive state X), overall detection efficiencies of $\sim$ 1 % and integrated luminosities of 100–200 pb^{-1}, only few events are expected at present in any of the several known decay channels of η_c; at least if the $\gamma\gamma$ width has the expected size of $\sim$ 5 keV[51]. Since hardly any mass distribution is free of background, the many upper limits obtained in the early years of PEP and PETRA operation had little significance [53]. The first measurement by the PLUTO collaboration[54] with only 45 pb^{-1} integrated luminosity and 7 observed events, without background, in the $K^\pm K^\circ_S\pi^\mp$ final state was therefore a surprise (Fig. 16 and Table 3). Later, the TASSO collaboration also reported a similar signal in the $K^\pm K^\circ_S\pi^\mp$ final state [57]. However, The Mark II group[55] and, this summer, the JADE group [56] do not confirm the high measured values of $\Gamma_{\eta_c\gamma\gamma}$, Figs. 17 and 18 and Table 3. Both the measurement of the R704 collaboration [58] using a H_2 gas jet target intersecting the cooled $\bar{p}$ beam in ISR (Fig. 19) and the upper limit from the missing mass measurement of the MD-1 group[59] (Fig. 20) seemed to indicate a value of $\Gamma_{\eta_c\gamma\gamma}$ in accordance with the theoretical expectations.

Experiment	Reaction	$\Gamma_{\eta_c\gamma\gamma}$ (keV)	Ref.
MD-1 (prel.)	$e^+e^- \rightarrow e^+e^-$ Miss.Mass	< 11 90 % C.L.	[59]
JADE (prel.)	$\gamma\gamma \rightarrow K^\pm K^\circ_S\pi^\mp$	< 11 95 % C.L.	[56]
TPC/2γ (prel.)	$\gamma\gamma \rightarrow$ 4-prongs	< 15 95 % C.L. > 1.6 95 % C.L.	[60] [60]
PLUTO	$\gamma\gamma \rightarrow K^\pm K^\circ_S\pi^\mp$	28 ± 15	[54]
Mark II *	$\gamma\gamma \rightarrow K^\pm K^\circ_S\pi^\mp$	8 ± 6	[55]
TPC/2γ (prel.)	$\gamma\gamma \rightarrow$ 4-prongs	$4.5\ ^{+5.5}_{-3.6}$	[60]
R704	$p\bar{p} \rightarrow \gamma\gamma$	$4.3\ ^{+3.4}_{-3.7} \pm 2.4$	[58]
World Average (weighted mean)		6 ± 3 keV	

* "In the absence of independent information concerning the shape of the background, one can ask if these 4 events are truly from η_c decays. However, since other experiments have reported signals, it would be remiss to only include upward fluctuations in the literature. Thus we quote a value rather than a limit."
G. Gidal, Berkeley 1986[55]

Table 3: Measurements of the $\gamma\gamma$ width of η_c. Where applicable, the BR($\eta_c \rightarrow K\bar{K}\pi$) from ref.[35] has been used.

New data are now presented by the TPC/2γ and TASSO collaborations. A complete analysis of the reaction $e^+e^- \rightarrow e^+e^-\eta_c$, $\eta_c \rightarrow$ 4-prongs has been made by the TPC/2γ group [60]. In this topology, η_c contributes with the decay channels $\eta_c \rightarrow 4\pi^\pm, K^+K^-\pi^+\pi^-$, $K^\pm K^\circ_S\pi^\mp$and $4K^\pm$. The latter channel consists of $\phi\phi$ as well as ϕK^+K^- and $K^+K^-K^+K^-$. Altogether these 4-prong decay modes constitute 4.5 % of η_c decays[2]. Only in the $4K^\pm$ decay mode a signal is seen, Fig. 21. Of the 4

[2]Only the $\phi\phi$ mode included from the $4K^\pm$ final state.

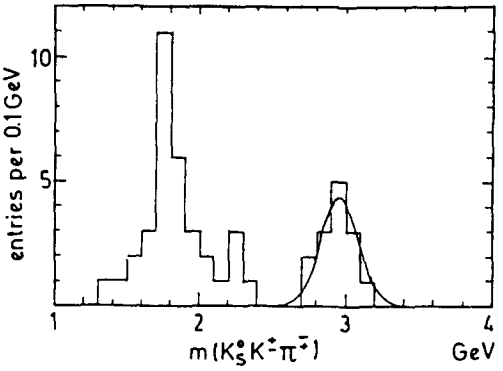

Figure 16: Inv. $K^{\pm}K^0_S\pi^{\mp}$ mass, 2 entries/ev. PLUTO data from 45 pb^{-1}. The curve shows the normalized η_c contribution.

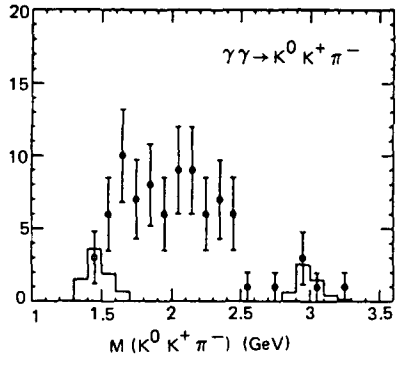

Figure 17: Inv. $K^{\pm}K^0_S\pi^{\mp}$ mass. Mark II data from 220 pb^{-1}. The curves show the normalized contributions from η_c and $\eta(1440)$.

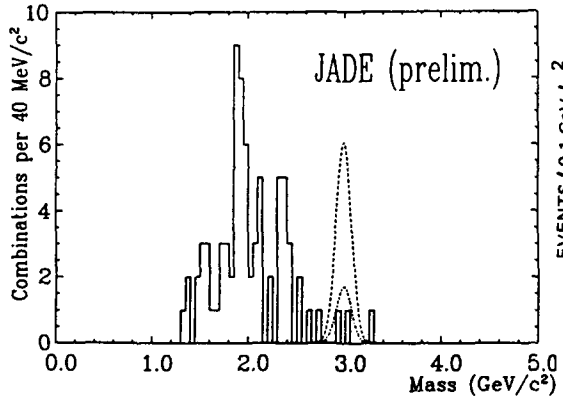

Figure 18: Inv. $K^{\pm}K^0_S\pi^{\mp}$ mass. JADE data from 224 pb^{-1}. The curves show the contributions from η_c, normalized to the PLUTO result (central value and -2σ).

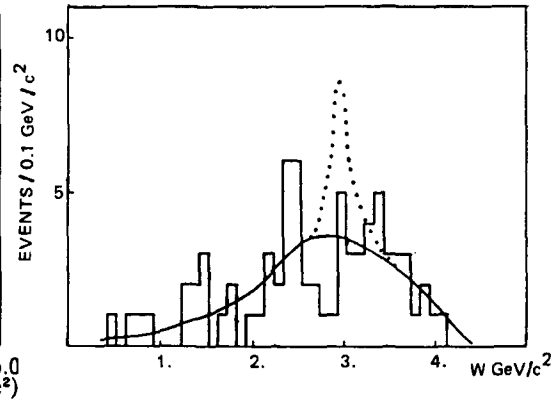

Figure 19: Missing mass in the reaction $e^+e^- \to e^+e^-X$. MD-1 data from 23.5 pb^{-1}. The full curve shows the expectation from non-resonant continuum, the dotted curve the η_c expectation for $\Gamma_{\eta_c\gamma\gamma}$=11 keV.

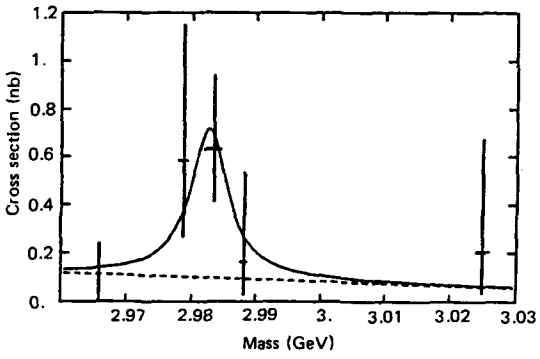

Figure 20: Excitation curve of $p\bar{p} \to \gamma\gamma$. Data from R704 coll. at ISR. The curves show the fitted contributions from η_c and background.

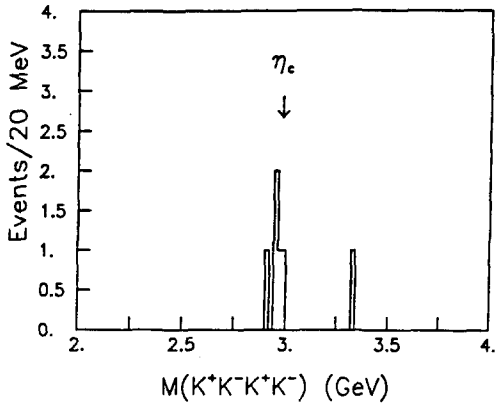

Figure 21: Inv. $K^+K^-K^+K^-$ mass. Data from TPC/2γ coll. with 70 pb^{-1}.

events attributed to η_c in this spectrum, one is of the type $\phi\phi$, and since BR($\eta_c \rightarrow \phi\phi$) is known, this establishes a *lower* limit for $\Gamma_{\eta_c\gamma\gamma}$(Table 3). The absence of signals in the other decay channels gives the upper limit and by combining all results, the measured value quoted in Table 3 is obtained.

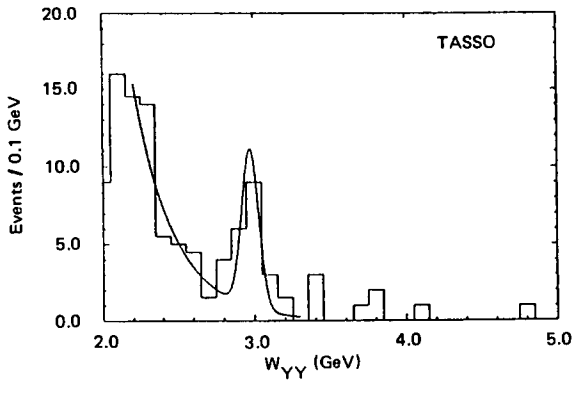

Figure 22: Inv. $K^{\pm}K^{\circ}_{S}\pi^{\mp}$ mass. TASSO data from 189 pb^{-1}. The curve shows the normalized η_c + background contribution.

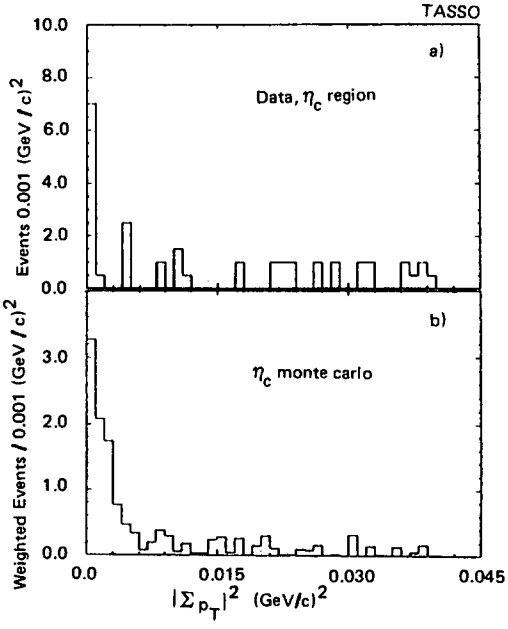

Figure 23: p_t^2 in the η_c region (2.75–3.2 GeV/c^2), for **a)** real data and **b)** MC simulation.

The analysis of the $K^{\pm}K^{\circ}_{S}\pi^{\mp}$ spectrum has been repeated by the TASSO group [61], with refined methods and much increased statistics. The $K^{\pm}K^{\circ}_{S}\pi^{\mp}$ mass spectrum is shown in Fig. 22. The intriguingly large signal (14±4 events) at the η_c mass remains. No measured value for $\Gamma_{\eta_c\gamma\gamma}$ is quoted yet, since there is an unclear point with the data, illustrated by the transverse momentum distributions in Figs. 23a and b. The real data seem to have too many events with large p_t values, a feature normally taken to indicate the presence of non-exclusive background, which however in this case also would have to contain an η_c component. Another possibility to be investigated is the influence of a possible J/ψ form-factor. It remains to be seen if further research into this interesting problem will resolve the apparent contradiction between the distributions of the "have's" in Figs. 16 and 22 on the one hand and of the "have not's" in Figs. 17 and 18 on the other hand.

The world average of the measurements in Table 3 is 6 ± 3 keV[3], which is in good agreement with the 5 keV expected from theory. Using this average value in the above relation, keeping only the 1st order term, one obtains

$$\alpha_s^{\overline{MS}}(m_{\eta_c}^2) \;=\; 0.21\,^{+0.05}_{-0.07}.$$

The large errors reflect also the present poor precision of $\Gamma(\eta_c \rightarrow hadrons)$, 11.5 ± 4.3 MeV[35]. The $\gamma\gamma$ widths of η_c and other pseudoscalars are calculated and discussed in a contributed paper[33].

Inclusive production of $D^{*\pm}$ mesons

In high p_t^{jet} multihadronic events resulting from $\gamma\gamma$ collisions charmed quarks are expected to contribute a large part. This is because the coupling of the two photons to the two quarks is proportional to the 4th power of the quark charge and because of the expected dominance of the box diagram contribution over the GVDM contribution at high p_t^{jet} values [62]. The measurement of charm production in multihadronic events can therefore be used to test the quark–parton model. Since the c–quark fragments preferentially into a $D^{*\pm}$ (2010) meson, the same method of charm identification

[3]Ironically, the effort of G. Gidal to "balance" the world average with the Mark II measurement now has the opposite effect, since the early TASSO measurement [57] is no longer quoted.

can be used as in the study of $D^{*\pm}$ production in annihilation events, namely the mass difference $\Delta m = m(D^{*\pm}) - m(D^{\circ})$ in the decay $D^{*\pm} \to \pi^{\pm} D^{\circ}$. This was first done by the JADE collaboration[63] using the decay $D^{\circ} \to K^{\mp}\pi^{\pm}\pi^{\circ}$ (BR=17.3%) in tagged multihadronic events. The Δm distribution is shown in Fig. 24a. The observed number of events, $19 \pm 7 \pm 3$, exceeds the QPM expectation of 3.4 ± 1.4. It was suggested that this excess could be due to QCD corrections to the box diagram, associated with 3- and 4-jet events[63,64].

The new data from the TPC/2γ collaboration[65] do not support this. The Δm distribution, using the decay $D^{\circ} \to K^{\mp}\pi^{\pm}$ (BR = 5.4%), is shown in Fig. 24b. Here the observed 8.1 ± 3.5 (4.0 ± 2.0) events are in good agreement with the QPM expectation of 7.5 (1.9) events for untagged and tagged events, respectively. Both groups are presently redoing their analyses with higher statistics and it remains to be seen if the excess observed by the JADE collaboration is confirmed or not.

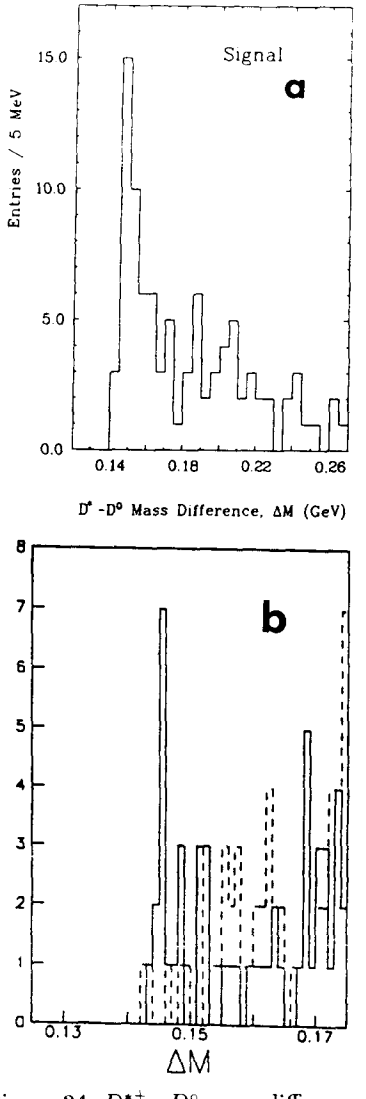

Figure 24: $D^{*\pm} - D^{\circ}$ mass difference in $\gamma\gamma$ multihadronic events.
a) Tagged JADE data from 90 pb^{-1}.
b) Prel. TPC/2γ data from 70 pb^{-1} (tagged and untagged). The dashed distribution shows the wrong sign combinations, i.e. $m(K^{\mp}\pi^{\pm}\pi^{\mp}) - m(K^{\mp}\pi^{\pm})$.

Production of spin = 1 mesons in $\gamma\gamma^*$ collisions

One of the most interesting topics in $\gamma\gamma$ physics at present is the discovery and study of the exclusive production of spin 1 resonances. Such formation can only take place if at least one of the photons is off mass shell, since 2 real photons can not couple to a spin 1 object. The discovery last year of a resonant state at a mass of ~ 1.4 GeV/c^2, observed in tagged exclusive $K^{\pm}K^{\circ}_S\pi^{\mp}$ events by the TPC/2γ collaboration [66], was soon confirmed by the Mark II group[55] and now also by the JADE collaboration [56]. Both TPC/2γ and Mark II have since updated their analyses[68,67]. The data are shown in Figs. 25a-c. The strongest argument for the spin 1 nature of the peak at 1.4 GeV/c^2 is its absence in the corresponding untagged event samples, as seen in the case of Mark II and JADE in Figs. 17 and 18 (slight differences in the cuts are not important for the present argument). For a meson with spin 0 or 2, a very large signal would be expected in the untagged samples, given the size of the tagged signals.

A similar observation is also reported by Mark II[15] and TPC/2γ[67] in the study of tagged exclusive $\eta\pi^+\pi^-$ events. The mass distributions are shown in Figs. 26a and b. Beside the η' peak a second peak is seen just below 1.3 GeV/c^2. Again there is no corresponding peak in the untagged events samples, as seen in the case of the Mark II data in Fig. 3, where only the η' shows up. Thus also here there is a strong case for the new resonant structure having spin 1.

Candidates for the two observed spin 1 structures are the well known meson resonances $f_1(1420)$ and $f_1(1285)$, formerly known as E(1420) and D(1285); these mesons both have the necessary positive C-parity. Both the TPC/2γ and Mark II groups have made efforts to establish this tentative assignment, although the scanty statistics allow only to demonstrate consistency.

The parity (both $f_1(1420)$ and $f_1(1285)$ have $J^{PC} = 1^{++}$) can be checked in several ways. A simple method has been

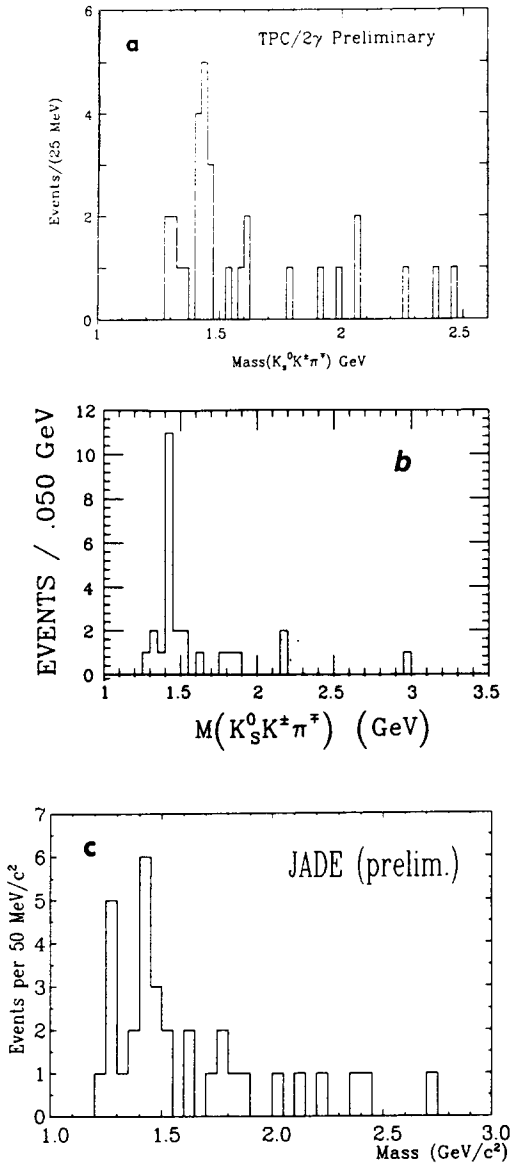

Figure 25: Inv. mass of $K^\pm K_S^0\pi^\mp$ in tagged events of the reaction $e^+e^- \to e^+e^- K^\pm K_S^0\pi^\mp$. **a)** TPC/2$\gamma$ data with 117 pb^{-1}, **b)** Mark II data with 220 pb^{-1}, **c)** JADE data with 213 pb^{-1}. The tagging ranges are 25–180, 21–83 and 32–75 mrad, respectively.

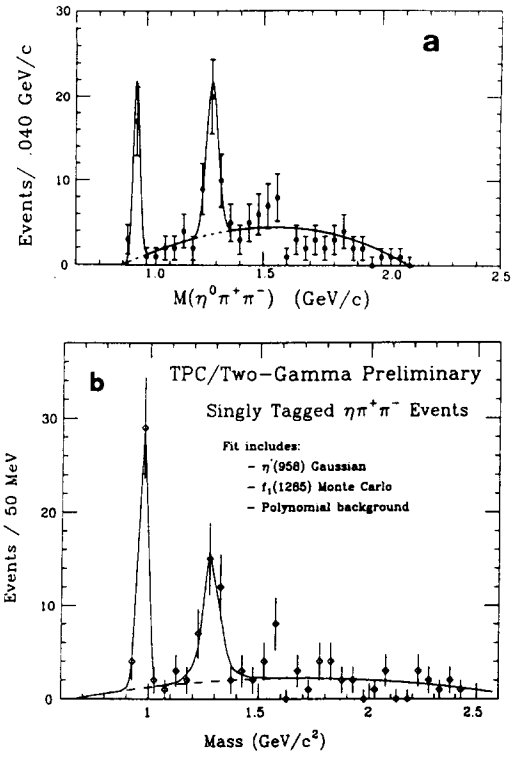

Figure 26: Inv. $\eta\pi^+\pi^-$ mass in tagged events of the reaction $e^+e^- \to e^+e^-\eta\pi^+\pi^-$. **a)** Mark II data with 220 pb^{-1}. The curves show fits to Gaussians and a polynomial background. **b)** TPC/2γ data.

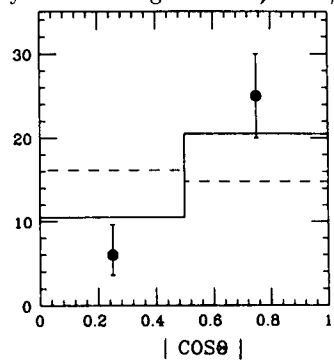

Figure 27: $|\cos\theta|$, with θ being the angle between incident photon and normal to decay plane in $\eta\pi^+\pi^-$ CM frame. Mark II data with m($\eta\pi^+\pi^-$) in band 1.22–1.34 GeV/c^2. The curves show expectations for $J^P = 1^+$ (solid) and $J^P = 1^-$ (dashed).

suggested by Cahn[69]: The distribution of $\cos\theta$, with θ being the angle between the incident photon and the normal of the decay plane, in the CM frame of the resonance, should, for small Q^2 values, be $1 \pm \cos^2\theta$ for $J^P = 1^\pm$. The Mark II analysis for the $\eta\pi^+\pi^-$ signal, shown in Fig. 27, favours the $J^P = 1^+$ assignment. In the case of the $K^\pm K^\circ_S \pi^\mp$ signal, the corresponding distribution (not shown) is not conclusive in either experiment, although TPC/2γ finds that $J^P = 1^+$ is favoured. The same conclusion is reached after a Dalitz plot analysis.

The production of a $J^{PC} = 1^{-+}$ state has been suggested by Chanowitz[70]. Such a state is exotic but could occur as a $q\bar{q}g$ hybrid (*meikton*), predicted in bag model calculations.

The $f_1(1420)$ meson has a dominant decay mode into K^*K[35]. Both Mark II and TPC/2γ find consistency with this decay mode in their Dalitz plots (not shown). $K^\pm K^\circ_S \pi^\mp$ is the only known dominant decay mode of the $f_1(1420)$. In the case of $f_1(1285)$, another major decay mode, beside $\eta\pi\pi$, is 4π (40%). The TPC/2γ group find in their $4\pi^\pm$ data (not shown) a weak signal, but it is not yet known whether the size is consistent with the $\eta\pi^+\pi^-$ signal.

The branching ratio of the decay $f_1(1285) \rightarrow K\bar{K}\pi$ is only 11 % and only few events are expected in the $K^\pm K^\circ_S \pi^\mp$ distributions. Here the JADE data in Fig. 25c are the most suggestive.

In the study of exclusive resonance production in $\gamma\gamma$ collisions, the measured quantity is $\Gamma_{X\gamma\gamma}$, the decay width of the resonance X into 2 photons. However, the really measured quantity is $\sigma(e^+e^- \rightarrow e^+e^- X)$, resulting after a suitable integration of

$$\frac{E_1' E_2' d^6\sigma}{d^3p_1' d^3p_2'} = \sum_{ij} \mathcal{L}_{ij}\sigma_{ij}$$

where E_1', E_2', p_1', p_2' are the energies and momenta of the scattered electrons and $\mathcal{L}_{ij}$ the photon flux factors[71,72,3]. The $\gamma\gamma$ couplings are given by σ_{ij}, for the virtual photons of polarization states i, j. $\Gamma_{X\gamma\gamma}$ is defined as a suitably normalized quantity, obtained in the limit $q_1^2 \rightarrow 0, q_2^2 \rightarrow 0$. The normalization is chosen so that agreement is obtained in the comparison with other methods of obtaining $\Gamma_{X\gamma\gamma}$, e.g. $\Gamma_{\pi^\circ\gamma\gamma}$ from a measurement of the π° lifetime.

In the case of spin 1 resonances such a definition does not apply, since the couplings are zero for the limit of real photons. However, if the q^2–dependences are known, one can factorize them out and thereby define constant quantities, which can serve as measures of the strength of the couplings. This is the approach of Cahn[69] who calls such a quantity $\tilde{\Gamma}$. The normalization of $\tilde{\Gamma}$ is a matter of convention. However, unlike the case of spin 0 and 2 resonances, no generally accepted convention exists for spin 1 resonances. In fact, the two groups that so far report quantitative results have adopted different conventions. These are briefly described in Fig. 28. As seen, the conventions differ by a factor 2 for $\tilde{\Gamma}$, although both groups use the non-relativistic quark model results of ref.[69] for describing $\Gamma_{\gamma\gamma^*}$ and for relating the LT and TT widths to the same constant $\tilde{\Gamma}$. It should be stressed that the latter relations are model dependent and that in fact the LT and TT widths are independent. Note also the difference in q^2–dependence for the 2 contributions; for small Q^2 the LT component dominates. The TT component is zero for all $q_1^2 = q_2^2$, in particular for the special case of $q_1^2 = q_2^2 = 0$. This is known as one of the Landau–Yang rules[73].

The convention used by TPC/2γ has the advantage that it is the same convention as is generally used for spin 0 and spin 2 mesons. Thus, in the limit $q_1^2 = q_2^2 = 0$, where only transverse polarized photons contribute, the cross section takes the well known approximate form (eq.3.24 in [72]):

$$\sigma_{\gamma\gamma} \approx 8\pi(2J+1)\frac{\Gamma\Gamma_{\gamma\gamma}}{(W^2 - M^2)^2 + M^2\Gamma^2}.$$

In the following, the results of the Mark II group for $\tilde{\Gamma}$ will be divided by 2 when comparing to the TPC/2γ results.

The results of the TPC/2γ and Mark II groups for $\tilde{\Gamma}_{f_1(1285)}$ and $\tilde{\Gamma}_{f_1(1420)}$ as well as the ratio $\tilde{\Gamma}_{f_1(1285)}/\tilde{\Gamma}_{f_1(1420)}$ are given in Table 4. The $\Gamma_{\gamma\gamma^*}$ Q^2–dependence for $f_1(1420)$, as measured by the

TPC/2γ convention

$$\sigma_{ij} = \frac{32\pi(2J+1)}{N_i N_j}\frac{W^2}{2\sqrt{X}}\frac{\Gamma\Gamma^{ij}_{\gamma\gamma^*}}{(W^2-M^2)^2+M^2\Gamma^2}$$

W is the CM energy of $\gamma\gamma$ system, M, Γ and J are the mass, total width and spin of the resonance and N_i is the number of polarization states for polarization i (1 for Longitudinal, 2 for Transverse polarization). X is defined by $X = (q_1 q_2)^2 - q_1^2 q_2^2 = \frac{1}{4}(W^2 - q_1^2 - q_2^2)^2 - q_1^2 q_2^2$.
By letting $W = M$ and performing the transition Breit-Wigner $\rightarrow$ δ-function, one obtains

$$\sigma_{ij} = \frac{32\pi(2J+1)}{N_i N_j}\frac{\pi M}{2\sqrt{X}}\delta(W^2-M^2)\Gamma^{ij}_{\gamma\gamma^*}$$

Thus,

$$2\frac{2\sqrt{X}}{M^2}\Gamma^{ij}_{\gamma\gamma^*(TPC/2\gamma)} = \Gamma^{ij}_{\gamma\gamma^*(MarkII)}$$

$$\Gamma^{LT}_{\gamma\gamma^*} = \frac{4X}{W^4}\frac{Q^2}{W^2}\tilde{\Gamma}F^2(q_1^2)F^2(q_2^2)$$

$$\Gamma^{TT}_{\gamma\gamma^*} = \frac{4X}{W^4}\left(\frac{q_1^2-q_2^2}{W^2}\right)^2\tilde{\Gamma}F^2(q_1^2)F^2(q_2^2)$$

Q^2 is the maximum of $|-q_1^2|, |-q_2^2|$. F is the ρ-pole:

$$F(q^2) = \left(1-\frac{q^2}{M_\rho^2}\right)^{-1}$$

Mark II convention

$$\sigma_{ij} = \frac{4\pi}{k^2}\frac{(2J+1)}{N_i N_j}\pi M\delta(W^2-M^2)\Gamma^{ij}_{\gamma\gamma^*}$$

k is the virtual photon momentum in the $\gamma\gamma$ CM system, with $k = \frac{\sqrt{X}}{M}$. This is eq. 4.10 in ref.[69], given in the narrow width limit of a Breit-Wigner form, i.e. at $W = M$. It is given only for the case of spin 1, i.e. for $ij = TT$ and LT (TL).

By substituting k, one obtains

$$\sigma_{ij} = \frac{32\pi(2J+1)}{N_i N_j}\frac{\pi M}{2\sqrt{X}}\frac{M^2}{4\sqrt{X}}\delta(W^2-M^2)\Gamma^{ij}_{\gamma\gamma^*}$$

$$\Gamma^{LT}_{\gamma\gamma^*} = \frac{k^3Q^2 8}{M^5}\tilde{\Gamma}F^2(q_2^2)$$

$$\Gamma^{TT}_{\gamma\gamma^*} = \frac{k^3Q^2 8}{M^5}\frac{Q^2}{M^2}\tilde{\Gamma}F^2(q_2^2)$$

These definitions correspond to eqs. 4.4 and 4.5, using 4.6, in ref.[69]. They are given for the limit $q_1^2 = 0$ and small $Q^2 = -q_2^2$.
Replacing k and using the above relations, with $W = M$, one obtains

$$2\frac{2\sqrt{X}}{M^2}\Gamma^{LT}_{\gamma\gamma^*(TPC/2\gamma)} = \Gamma^{LT}_{\gamma\gamma^*(MarkII)} = \frac{4X}{M^4}\frac{Q^2}{M^2}\frac{2\sqrt{X}}{M^2}\tilde{\Gamma}_{(MarkII)}F^2(q_2^2)$$

and a similar relation for the TT combination. Thus,

$$2\tilde{\Gamma}_{(TPC/2\gamma)} = \tilde{\Gamma}_{(MarkII)}$$

Figure 28: Conventions used in the definition of $\Gamma_{\gamma\gamma^*}$ for spin 1 resonances.

TPC/2γ group, is shown in Fig. 29a and the Mark II results for $f_1(1285)$ and η' are shown in Fig. 29b. Note that Fig. 29a shows $\Gamma_{\gamma\gamma^*} = \Gamma^{LT}_{\gamma\gamma^*} + \frac{1}{2}\Gamma^{TT}_{\gamma\gamma^*}$ as function of Q^2, while Fig. 29b shows the constants $\tilde{\Gamma}_{f_1(1285)}$ and $\Gamma_{\eta'\gamma\gamma}$, calculated in two different Q^2-ranges. The η' results are obtained by assuming the ρ-pole for the Q^2-dependence. Note that the latter results are obtained with the "standard" convention and not the one used for spin 1 in Fig. 28.

Experiment	$\tilde{\Gamma}_{f_1(1285)}$ (keV)	$\tilde{\Gamma}_{f_1(1420)}$ BR($K\bar{K}\pi$) (keV)	$\frac{\tilde{\Gamma}_{f_1(1285)}}{\tilde{\Gamma}_{f_1(1420)}\mathrm{BR}(K\bar{K}\pi)}$	Ref.
TPC/2γ (prel.)	< 2.4 (90 % c.l.)	$1.3 \pm 0.5 \pm 0.3$	< 2.5 (90 % c.l.)	[67]
Mark II	$4.7 \pm 1.25 \pm 0.85$	$1.6 \pm 0.7 \pm 0.3$	2.9 ± 1.5	[15,68]

Table 4: Measurements of $\tilde{\Gamma}$ for spin 1 resonances. The Mark II measurements have been divided with 2.

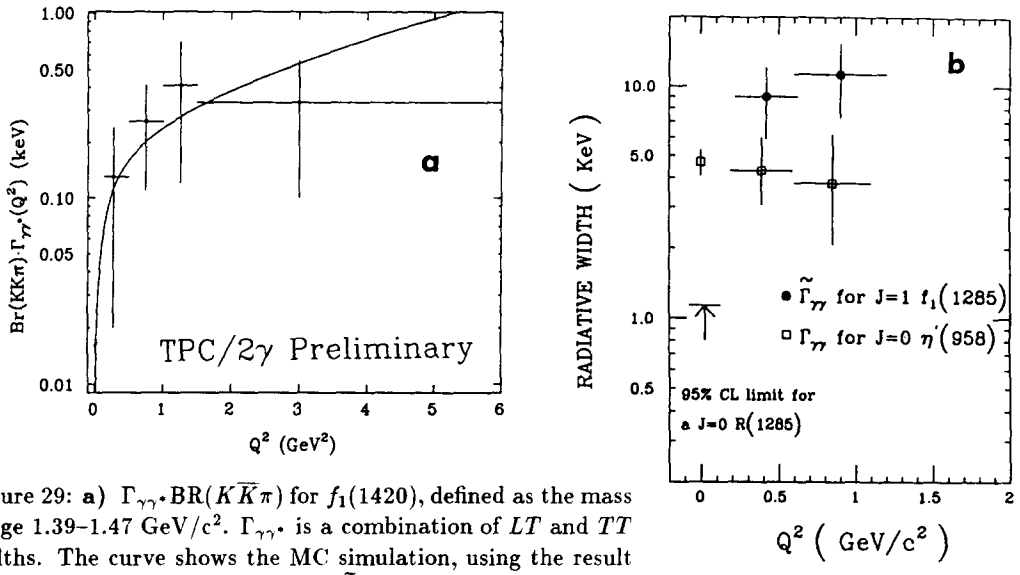

Figure 29: **a)** $\Gamma_{\gamma\gamma^*}$·BR($K\overline{K}\pi$) for $f_1(1420)$, defined as the mass range 1.39–1.47 GeV/c^2. $\Gamma_{\gamma\gamma^*}$ is a combination of LT and TT widths. The curve shows the MC simulation, using the result in Table 4. **b)** Mark II results for $\tilde{\Gamma}_{f_1(1285)}$ and $\Gamma_{\eta'\gamma\gamma}$.

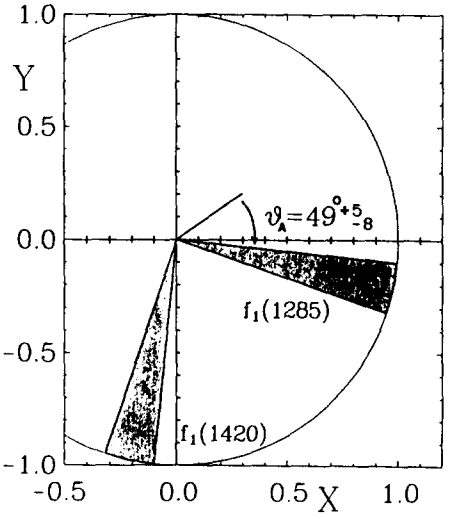

Figure 30: Rosner plot for axial vectors.

There is reasonable agreement between the two groups in their results, as given in Table 4, although there is a slight discrepancy in the measured rate of $f_1(1285)$. The TPC/2γ result for $f_1(1285)$ is based on the analysis of the $K^{\pm}K^0_S\pi^{\mp}$ and $4\pi^{\pm}$ data samples; the analysis for the spectrum in Fig. 26b is underway. One can of course now speculate whether the assignment of the observed signals to $f_1(1285)$ and $f_1(1420)$ is really correct. This can only be established with much larger statistics.

Assuming that it *is* correct, we can continue with the speculations. Both these resonances are normally assigned to the axial vector SU(3) nonet, with the remaining members being the $a_1(1270)$ and $K_A(1340)$ (a C-even mixture of $K_1(1280)$ and $K_1(1400)$). The quadratic mass formula gives the mixing angle θ_A = 42.2°, which is rather close to the ideal mixing value (35.26°). That $f_1(1420)$ is almost pure $s\bar{s}$ is supported by the only seen decay to $K\overline{K}\pi$ (K^*K) while $f_1(1285)$ decays mainly to $\eta\pi\pi$ and 4π. It is now interesting to see if the measured $\gamma\gamma$ widths agree with this. With the additional assumptions of nonet symmetry and s–wave phase space, one can write

$$\frac{\tilde{\Gamma}_{f_1(1285)}}{\tilde{\Gamma}_{f_1(1420)}} = \frac{M_{f_1(1285)}}{M_{f_1(1420)}} \left(\frac{\sin\theta_A + \sqrt{8}\cos\theta_A}{\sqrt{8}\sin\theta_A - \cos\theta_A} \right)^2 .$$

Using the measured ratio of the Mark II group and assuming 100 % BR($f_1(1420)\rightarrow K\overline{K}\pi$), one finds $\theta_A = 49^{+5\,\circ}_{-8}$, in good agreement with the quadratic mass formula value and not far from the ideal mixing value. The result is shown in the Rosner plot in Fig. 30. Although this looks fine, it must be stressed that many assumptions are involved, also in deriving the formulas used in obtaining the

measurements of $\tilde{\Gamma}_{f_1(1285)}$ and $\tilde{\Gamma}_{f_1(1420)}$. When using the upper limit from TPC/2γ for the ratio, θ_A assumes values much farther from ideal.

It has been pointed out[4] that the data obtained by the LASS spectrometer group [74] on the reaction $K^- p \rightarrow K^{\pm} K^0_S \pi^{\mp} \Lambda$ make the assignment of $f_1(1420)$ to the $s\bar{s}$ member of the axial vector nonet unlikely. The data of this reaction, which is expected to produce strangeonia, do not show production of $f_1(1420)$, but instead another $J^{PC} = 1^{++}$ state at ~ 1.53 GeV/c^2.

Vector Meson pair production

A vector meson, having the quantum numbers of the photon, $J^{PC} = 1^{--}$, can be considered as being "heavy light". A natural approach to the virtual $\gamma\gamma$ scattering is therefore to consider it in terms of vector meson interactions. Based on this approach, known as the Vector Dominance Model (VDM), and the early results in photoproduction, the diffractive scattering of ρ-mesons on ρ-mesons was considered already in the end of the 1960s[75]. Indeed, Budnev et al.[76] predicted, by use of the factorization theorem, the cross section for $\rho\rho$ production, $\sigma(\gamma\gamma \rightarrow \rho^0\rho^0)$, to be of the size 20–50 nb, at $W_{\gamma\gamma}$ above 1 GeV.

The first measurement of $\rho^0\rho^0$ production was made by the TASSO collaboration in 1980 [77] and the cross section was found to be even higher than the early prediction, namely ~ 100 nb at ~ 1.5 GeV. Other groups have confirmed this high value[78]. In Fig.31 the latest measurement, presented by PLUTO [79] this summer, is shown. The early efforts to explain this high cross section in terms of resonance production were disproved in 1983 by the JADE limits[80] on the corresponding reaction $\gamma\gamma \rightarrow \rho^+\rho^-$, also shown in Fig.31. The cross section for $\rho^+\rho^-$ production would be a factor 2 (I=0) or 1/2 (I=2) times $\sigma(\gamma\gamma \rightarrow \rho^0\rho^0)$, in case of single resonance production. Two models remained that were able to explain these cross sections: the *t-channel factorization model* by Alexander et al.[81] and the *4-quark resonance model* by Achasov et al.[82] and by Li and Liu[83]. These models are also shown in Fig.31. In the latter model the suppression of $\sigma(\gamma\gamma \rightarrow \rho^+\rho^-)$ is predicted by the destructive interference of I=0 and I=2 resonances of about the same mass; constructive interference in the case of $\rho^0\rho^0$ decay produces a high cross section.

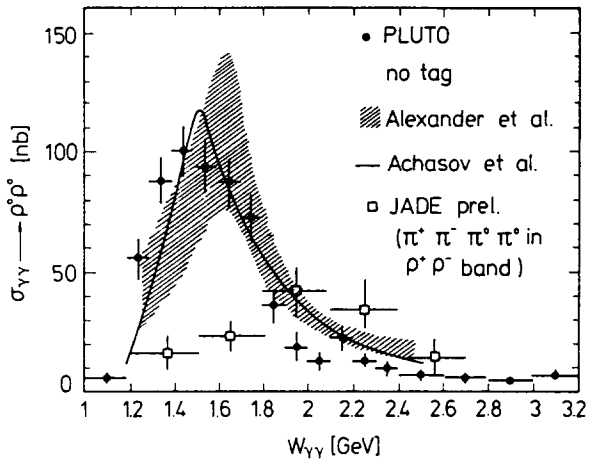

Figure 31: Cross section $\sigma(\gamma\gamma \rightarrow \rho\rho)$. PLUTO data for $\gamma\gamma \rightarrow \rho^0\rho^0$ and prel. JADE data for $\gamma\gamma \rightarrow \rho^+\rho^-$.

Both these approaches were used for further predictions about the size of similar reactions involving other pair combinations of vector mesons: $\gamma\gamma \rightarrow \rho^0\omega$, $\gamma\gamma \rightarrow \omega\omega$, $\gamma\gamma \rightarrow \rho^0\phi$, $\gamma\gamma \rightarrow \phi\phi$ and $\gamma\gamma \rightarrow K^{*0}\overline{K^{*0}}$. New measurements and stringent limits on these processes are presented this summer by the ARGUS and TPC/2γ groups, and can be used to test the model predictions.

The ARGUS collaboration have now finalized their preliminary measurement from 1986 of the reaction $e^+e^- \rightarrow e^+e^-\rho^0\omega$ [84]. A new, preliminary measurement is also presented by the TPC/2γ group at this conference [85]. The results are shown in Fig. 32 and are in good agreement with each other. They are also consistent with the earlier upper limits on this reaction (PLUTO[86] and JADE[87], not shown).

The present measurements show that the cross section $\gamma\gamma \rightarrow \rho^0\omega$ rises to a maximum at $W_{\gamma\gamma} = 1.9$–2.0 GeV, with a rapid fall off at higher mass values. None of the quoted models predicts this behaviour. The ARGUS group have made a spin-parity analysis of their data (considering $J^P = 0^+, 0^-, 2^+, 2^-$),

[4] I thank B. Ratcliff for drawing my attention to these data after the talk.

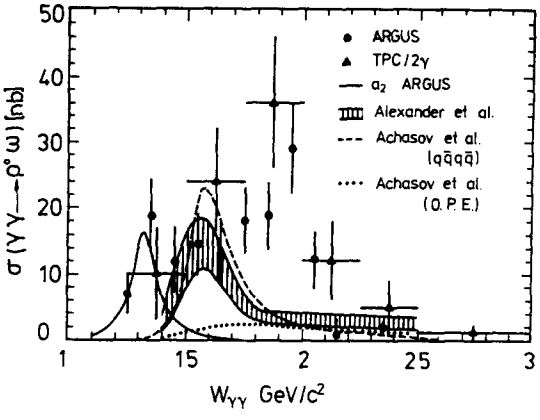

Figure 32: Cross section $\sigma(\gamma\gamma \to \rho^0\omega)$. ARGUS and preliminary TPC/2γ data from 234 and 64 pb^{-1}, respectively. Additional systematic errors are quoted at +16, −30 % (ARGUS) and ±28 % (TPC/2γ).

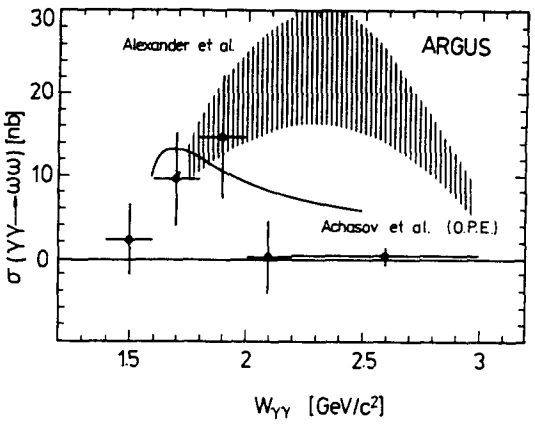

Figure 33: Cross section $\sigma(\gamma\gamma \to \omega\omega)$. ARGUS data from 234 pb^{-1}. Additional systematic errors are quoted at ±20 %.

with the result that no particular spin-parity value dominates, the relevant angular distributions are compatible with isotropy or with a mixture of several spin-parity or helicity states. Thus the production of a single resonance with mass = 1.9–2.0 GeV/c^2, decaying to $\rho^0\omega$, seems improbable.

In a contribution to the conference [88], estimates of the one pion exchange (OPE) contributions to the processes $\gamma\gamma \to \rho^0\omega$ and $\gamma\gamma \to \omega\omega$ are given. It is suggested that such contributions could interfere with the production of q$\bar{\text{q}}$q$\bar{\text{q}}$ states, and thereby shift the mass. This calculation is also shown in Fig. 32, with the Regge slope parameter B = 1.0.

The reaction $\gamma\gamma \to \omega\omega \to 6\pi$ offers formidable experimental problems in terms of combinatorial background (there are 8 $\pi^+\pi^-\pi^0$ combinations in each event, but only 2 ω) and demands on resolution. The ARGUS group [89] now presents the first measurement of this process, of which only upper limits existed so far (PLUTO[86] and JADE [87]). The measured cross section, based on 29 events above background, is shown in Fig. 33. It exhibits the same feature as the previous $\sigma(\gamma\gamma \to \rho^0\omega)$, namely a fast rise to the maximum at $\sim$ 1.9 GeV and then a rapid fall off. Again, the quoted models fail to describe the observed behaviour. While the factorization model predicts too much at too high $W_{\gamma\gamma}$, the q$\bar{\text{q}}$q$\bar{\text{q}}$ model does not expect an enhancement in this channel. The OPE calculation, with B = 1.0, is however in rough agreement.

The final state topology $K^+K^-\pi^+\pi^-$ occurs in both the reactions $\gamma\gamma \to K^{*0}\overline{K^{*0}}$ and $\gamma\gamma \to \rho^0\phi$. Limits on the cross sections were given by the TASSO [90] and TPC/2γ [91] groups. The former reaction has now been observed and measured for the first time by the ARGUS group [92]. The cross section, based on 41 events above background, is shown in Fig. 34 together with model predictions. The size and shape is not predicted by the q$\bar{\text{q}}$q$\bar{\text{q}}$ model. The model by Brodsky, Köpp and Zerwas [93], which is based on perturbative QCD applied in a "dual picture between perturbative QCD and resonance production near threshold", gives predictions for $\gamma\gamma \to K^*\overline{K^*}$ as well as for $\gamma\gamma \to \rho^+\rho^-, D\overline{D}$ and $D^*\overline{D^*}$. It is also shown in Fig. 34; the large rise of the measured σ at $\sim$ 2 GeV is not explained.

Finally, the ARGUS group [92] have used their data to set new limits on the production of $\rho^0\phi$ in $\gamma\gamma$ collisions. That the q$\bar{\text{q}}$q$\bar{\text{q}}$ model has great problems in this channel was already clear with the limits set by the TPC/2γ group [91]. The factorization model expects this reaction to appear at the level of, or below, the present ARGUS limit of 0.5 nb at 95 % c.l. The present limits and the q$\bar{\text{q}}$q$\bar{\text{q}}$ model predictions are shown in Fig. 35.

From the above one concludes that the rich amount of new data in vector meson pair production is

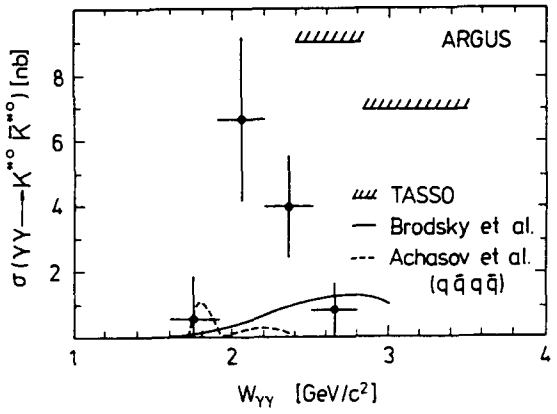

Figure 34: Cross section $\sigma(\gamma\gamma \to K^{*\circ}\overline{K^{*\circ}})$. Data from ARGUS corresponding to 234 pb^{-1}.

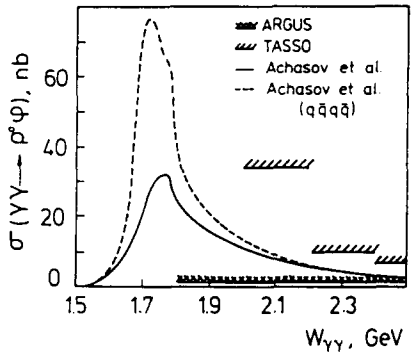

Figure 35: Cross section $\sigma(\gamma\gamma \to \rho^\circ\phi)$ with upper limits from TASSO and ARGUS. Upper limits from TPC/2γ practically coincide with the ARGUS limits. The curves represent predictions from the $q\bar{q}q\bar{q}$ model, for 2 choices of parameters.

largely not understood in the theory. The approach of the factorization model seems to describe data in the purely diffractive channels: $\gamma\gamma \to \rho^\circ\rho^\circ$, $\gamma\gamma \to \rho^\circ\phi$ and $\gamma\gamma \to \phi\phi$, of which only $\gamma\gamma \to \rho^\circ\rho^\circ$ is measured so far. It fails however in describing non-diffractive channels like $\gamma\gamma \to \rho^\circ\omega$ and $\gamma\gamma \to \omega\omega$. It should be remembered that this model is really a phenomenological method of relating $\gamma\gamma$ production with photoproduction:

$$\sigma(\gamma\gamma \to \rho^\circ\rho^\circ) = \frac{\sigma^2(\gamma p \to \rho p)}{\sigma(pp \to pp)} \frac{F_{\gamma p}^2}{F_{pp} F_{\gamma\gamma}}$$

with the F's being flux factors. This method may not work well for non-diffractive (π-exchange) channels and is moreover sensitive to the quality of the input data from photoproduction. The approach of factorization has been criticized in a contribution to this conference[94].

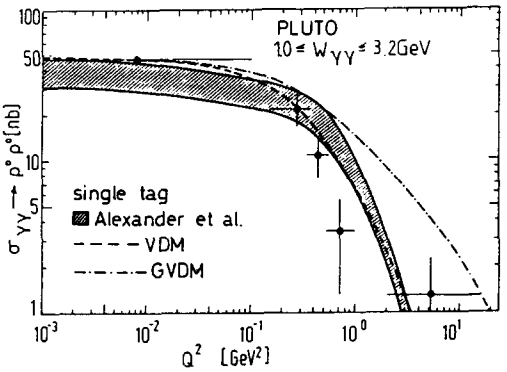

Figure 36: Cross section $\sigma(\gamma\gamma \to \rho^\circ\rho^\circ)$ for finite Q^2 (tagged events). PLUTO data from to 45 pb^{-1}. The tagging range is 23–60, 85–300 mrad.

The $q\bar{q}q\bar{q}$ model has so far given a number of predictions in various channels, which, except for the case of $\rho\rho$, fail to describe the present data. Since the model has several parameters to "tune", one would like to see the model being applied in a global adjustment of these parameters to all available data, in order to possibly bring out a consistent picture in this interesting approach to the explanation of vector meson pair production.

This section is finished with a presentation of new data on single tagged production of $\rho^\circ\rho^\circ$. A measurement by the PLUTO [79] group is shown in Fig. 36. Single tagged production of $4\pi^\pm$ has also been measured by the TPC/2γ [95] and TASSO [96] groups. In the latter case, $\rho^\circ\rho^\circ$ production is estimated to $\sim$ 50 % of the $4\pi^\pm$ cross section and agrees well with the measurement in Fig. 36. The data follow nicely a ρ-pole description. It is interesting to note that the factorization model describes $\rho^\circ\rho^\circ$ production well also at finite Q^2.

The photon structure function F_2^γ

The pointlike part of the hadronic photon structure function F_2^γ is calculable in QCD [97] and offers, in leading order, a measure of $\Lambda_{\overline{MS}}$:

$$F_2^{\gamma,LO} \sim \frac{1}{\alpha_s} \sim \ln \frac{Q^2}{\Lambda^2_{\overline{MS}}}$$

This relation has spurred much experimental work, since F_2^γ can be measured at e^+e^- storage rings, via deep inelastic $e\gamma$ scattering. An impressive body of experimental data has been accumulated since the first measurement in 1981 [98,99,100] and covers now a Q^2-range of 0.2 - 300 $(GeV/c)^2$. Data have clearly borne out the predicted increase of F_2^γ with increasing Q^2, as well as the predicted absolute normalization. Moreover, the peaking of F_2^γ at high values of x has clearly been seen, with the scaling variable x defined in terms of Q^2 and the $\gamma\gamma$ mass $W_{\gamma\gamma}$: $x = Q^2/(Q^2 + W^2_{\gamma\gamma})$.

Due to limited acceptance, in general $W_{measured} \leq W_{true}$. MC methods have to be used to derive the corresponding true x-distribution from the measured $x_{vis.}$-distribution. Refined software methods have been developed for this purpose and unfolding can now be considered a "standard treatment" in the analysis of F_2^γ. With one exception all groups have even used the same unfolding program [101]. This is also true for the two new analyses presented at this conference.

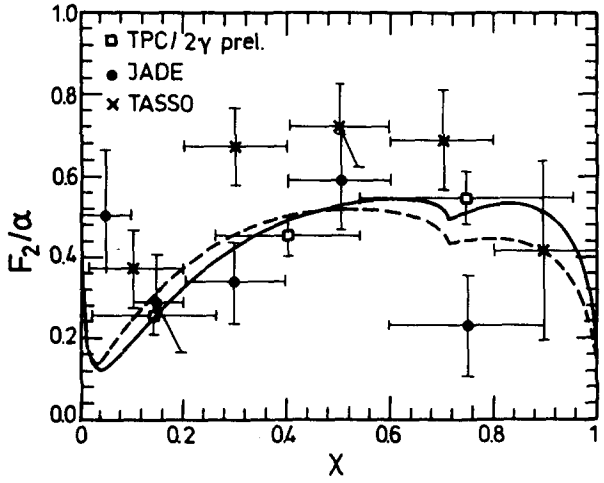

Figure 37: Measured unfolded structure function F_2^γ. Data from TPC/2γ, JADE and TASSO with $\langle Q^2 \rangle$ = 22.4, 24 and 23 $(GeV/c)^2$, respectively. The curves show adjustments of the regularised calculation in ref.[103].

The TPC/2γ collaboration have extended their previous F_2^γ analysis at low Q^2 (0.2 - 7 $(GeV/c)^2$) [99,100] to a range of high Q^2, 10 - 60 $(GeV/c)^2$ [102], using the pole tip calorimeters to measure the scattered electrons. The unfolded x-distribution is shown in Fig. 37, with $\langle Q^2 \rangle$ = 22.4 $(GeV/c)^2$. Previous data from JADE and TASSO with similar $\langle Q^2 \rangle$ are also shown. The agreement is acceptable, although it seems that systematic errors may be underestimated.

The TPC/2γ data have been analysed using the regularised higher order calculation of F_2^γ given by Antoniadis and Grunberg [103]. This is by now also a "standard" procedure, followed by most experimental groups. The regularised calculation expresses F_2^γ as

$$F_2^\gamma(x, Q^2) = F_2^{reg}(x, Q^2; \Lambda_{\overline{MS}}) + \Delta(x, t) + F_2^{had}(x),$$

where the pointlike F_2^{reg} keeps the sensitivity to $\Lambda_{\overline{MS}}$ for x values $\geq$ 0.4. The new variable t in the regularisation term Δ is not calculable for a real photon target (it is calculable for virtual photon target) but can be determined by the data; since sensitivity to t is mainly in the low x region, the $\Lambda_{\overline{MS}}$ determination is not much affected. The c-quark contribution is in this Q^2-range still subject to a mass threshold effect and has only small QCD corrections. Therefore, and this is also standard treatment, its contribution is estimated using the QPM calculation [72].

In Fig. 37 the two curves show the adjustment of this regularised calculation to the TPC/2γ data. The curves differ in the treatment of the hadronic piece, F_2^{had}, assuming upper and lower limits of this contribution. The lower limit is simply given by $F_2^{had} = 0$. For the upper limit estimate, the TPC/2γ

group have used their own previous measurement of F_2^{had}[100] at low Q^2. In this measurement it was found that the standard parametrisation, $F_2^{had} = 0.2\alpha(1-x)$, which is derived from the pion structure function[104,105] and used in previous analyses, is a good description at higher x; at low x however, the data fall below this line. The hadronic piece is predicted in QCD[106] to decrease slowly with increasing Q^2. By using the Q^2 evolution given in [106] for hadronic targets the maximum contribution of F_2^{had} at $\langle Q^2 \rangle = 22.4$ (GeV/c)^2 was obtained from this low Q^2 measurement. This treatment of F_2^{had} removes one uncertainty present in previous analyses.

The adjustment of the regularised calculation to the TPC/2γ data leads to a determination of $\Lambda_{\overline{MS}}$:

$$119 \pm 34 < \Lambda_{\overline{MS}} < 215 \pm 55 \text{ MeV}.$$

This compares well to the weighted mean value of $\Lambda_{\overline{MS}}$ obtained from previous measurements of F_2^γ, $\Lambda_{\overline{MS}} = 195^{+60}_{-40}$ MeV [107].

The measurement of $\Lambda_{\overline{MS}}$ using the F_2^γ data has a remarkable precision, in fact it is one of the most precise measurements; it agrees well with the $\Lambda_{\overline{MS}}$ values obtained in other measurements [108]. This sensitivity to $\Lambda_{\overline{MS}}$ in the F_2^γ data is since years the subject of theoretical dispute. It stands in apparent contrast to the expected smallness, at Q^2 values within experimental reach, of the QCD corrections to the naive (non-interacting) QPM [109]. Indeed, the scale-breaking rise of F_2^γ with $\ln(Q^2)$ and the peaking at high x is also predicted in the QPM description [72] and several groups find that QPM gives an equally good description of the data. In this case Λ is replaced by quark masses. It has been argued [110] that since quark masses of 300 and 500 MeV (u,d and s) are needed to describe the data with QPM, one sees here a QCD effect, "dressing" the quarks.

The theoretical discussion in recent years has concentrated on the separation of F_2^γ into the pointlike part F_2^{PL}, coming from the interaction of the probe-photon with one of the quarks in the split target photon, and F_2^{had} from the interaction with the hadronic part of the target photon. In higher order calculations of F_2^γ, the separation of F_2^γ into $F_2^{PL} + F_2^{had}$ creates unphysical poles in both parts. The cancellation of these poles leads to the regularised solution above. Double counting of the hadronic part between the regularisation term Δ and F_2^{had} cannot be excluded and some groups took this into account in the analysis by a third adjustable parameter h, multiplying F_2^{had}.

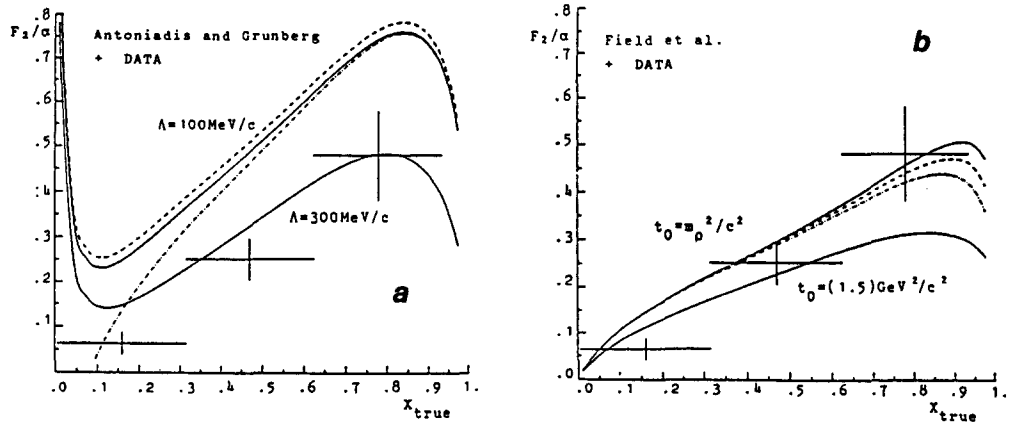

Figure 38: Measured unfolded structure function F_2^γ. CELLO data from 35 pb^{-1} and with $\langle Q^2 \rangle = 17$ (GeV/c)^2. **a)** two values of $\Lambda_{\overline{MS}}$ and 3 values of t: $t = .1$ (full line), $t = 1$ (dashes), $t = 0$ (dot-dashes). **b)** two values of t_0 and 3 values of Λ: $\Lambda = 50$ MeV/c (full line), $\Lambda = 150$ MeV/c (dashes), $\Lambda = 300$ MeV/c (dot-dashes).

This approach has been strongly criticized by Field et al. [111]. In their calculation of F_2^{PL}, a physically sound motivation for the separation of F_2^γ into pointlike and hadronic pieces is given,

namely the onset of high p_t jet formation from the pointlike interaction[104]. In the perturbative calculations a lower cut-off in the squared momentum transfer, t_o, is therefore applied. This leads to the replacement of $\ln(Q^2/\Lambda^2)$ with $\ln(Q^2/t_o)$ in the leading log term and the dependence on Λ is relegated to non-leading log (NLL) terms, in all orders of α_s. The sensitivity to Λ is overshadowed by the $\ln(Q^2/t_o)$ term, i.e. by non-perturbative effects. t_o can in principle be determined from the data, e.g. by studies of jet structure in the final state, and is expected to take values from $\sim m_\rho^2$ to 1-2 $(GeV/c)^2$, i.e. larger than the $\Lambda_{\overline{MS}}$ value found above.

Thus Field et al. arrive at a separation of F_2^γ into a pointlike and a hadronic part, both of which are free of unphysical poles. They stress that NLL terms are important at all orders. The neglect or misinterpretation of these terms in other approaches is the cause of artificial singularities. This is also in agreement with the results reached in refs.[97,112].

The CELLO group[113] presents a new analysis of F_2^γ based on data from 35 pb^{-1}, at $\langle Q^2 \rangle = 17$ $(GeV/c)^2$. The unfolded x-distribution is shown in Fig. 38. The analysis has been performed using both the regularised calculation by Antoniadis and Grunberg and the new calculation by Field et al.. The sensitivity to Λ and to t, at high and low x respectively, in the first approach, is clearly seen in the curves of Fig. 38a. In contrast, Fig. 38b shows the sensitivity to the cut-off parameter t_o, and the corresponding insensitivity to Λ. A t_o value of $\sim m_\rho^2$ seems to agree well with the data.

The conclusions of Field et al. have recently been modified by Frazer [114], who presented calculations which indicate that part of the sensitivity to Λ is restored at experimentally accessible Q^2 and at large values of x. Thus, for $Q^2 = 45$ $(GeV/c)^2$, $x = 0.9$ and $t_o = 0.5$ $(GeV/c)^2$, 47 % sensitivity is expected. However, it should be remembered that the bulk of the present data is found at lower x values and at much lower Q^2 values.

In the analysis of the low Q^2 data [99,100] the TPC/2γ group concluded that scaling is observed in the lowest x-bin of 0.-0.1, with F_2^γ being constant over the Q^2 range of 0.3 - 7 $(GeV/c)^2$. In contrast, F_2^γ was found rising with Q^2 in higher x-bins. The data are shown in Fig. 39. The interpretation of scaling is criticized in a contribution [115] to the conference. It is argued that the constancy is accidental and due to averaging over large $W_{\gamma\gamma}$-intervals. This may be a valid objection considering the nonlinear dependence of x on $W_{\gamma\gamma}$. To demonstrate scaling of F_2^γ at low x-values, a finer binning in x ought to be used.

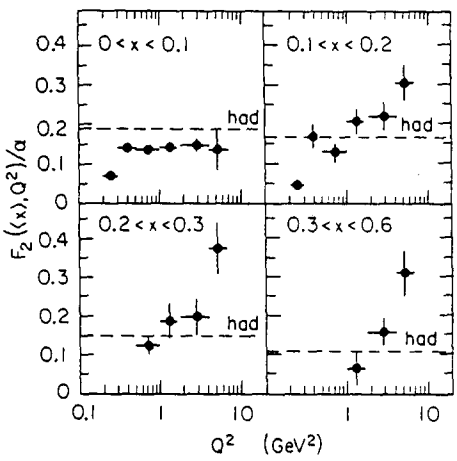

Figure 39: Measured unfolded structure function F_2^γ, as function of Q^2 in 4 bins of x. The dashed line shows the hadronic component, $0.2\alpha(1-x)$. Data from TPC/2γ.

Summary

The measured $\gamma\gamma$ widths of pseudoscalars and tensors have now reached a high precision. For the pseudoscalars, a consistent picture of decay rates and the SU(3) isoscalar mixing angle can be obtained; the mixing angle is large and negative and there is no need for additional gluonic matter in this nonet. Radial excitations of the pseudoscalar nonet have not been seen, with significant limits.

The measured mean value of $\Gamma_{\eta_c\gamma\gamma}$ is 6 ± 3 keV, in good agreement with theory. Discrepancies between experiments need to be clarified. This is also true for inclusive $D^{*\pm}$ production, where one group found agreement with the QPM expectation and another group measured an excess over this expectation.

The study of spin 1 production (possibly axial vectors) in tagged $\gamma\gamma^*$ collisions has emerged as a new rich field in $\gamma\gamma$ physics. Much more data will be required to resolve the many questions raised by

the presently available data. Agreement on the definition of $\Gamma_{\gamma\gamma}$ is desirable.

The production of vector meson pairs in $\gamma\gamma$ collisions needs theoretical understanding. More data will bring light on the possible resonant nature of the threshold enhancements observed in $\gamma\gamma \to \rho^0\omega$, $\gamma\gamma \to \omega\omega$ and $\gamma\gamma \to K^{*0}\overline{K^{*0}}$.

An excellent measurement of $\Lambda_{\overline{MS}}$ exists, obtained in the study of the hadronic photon structure function F_2^γ. There is no theoretical agreement on whether this measurement makes sense or not.

Acknowledgements

I wish to thank all the groups for providing the vast amount of new data on $\gamma\gamma$ physics. I am deeply thankful for all the help I received in preparing the talk as well as these proceedings, by numerous colleagues at DESY and elsewhere. In particular I want to mention A. Eisner, F. Erné, M. Feindt, J. Field, G. Gidal, E. Gotsman, P. Hill, A. Levy, U. Maor, H. Marsiske, S. Maxfield, A. Nilsson and M. Poppe. Warm thanks are also due to the organizers of the conference and last, not least, to my efficient scientific secretary, M. Kuhlen.

References

[1] Ch. Berger and W. Wagner, Phys.Rep.**146**(1987)1.
[2] Proc. VIIth Intern. Workshop on Photon-Photon Collisions, Paris, 1986.
[3] M. Poppe, Intern. Journ. Mod.Phys.**A1**(1986)545.
[4] D. Williams, Thesis, Harvard 1987, unpubl.
[5] F. Low, Phys.Rev.**120**(1960)582.
[6] H. Atherton et al., Phys.Lett.**158B**(1985)81.
[7] G. Bellettini et al., Nuovo Cimento **66A**(1970)243; V. Kryshkin et al., JETP **30**(1970)1037;
A. Browman et al., Phys.Rev.Lett.**33**(1974)1400.
[8] C. Bemporad et al., Phys.Lett.**25B**(1967)380; A. Browman et al., Phys.Rev.Lett.**32**(1974)1067.
[9] S. Cooper, Proc. 23rd Int. Conf. on High Energy Physics, Berkeley, 1986.
[10] M. Zieliński, Acta Phys.Pol.**B18**(1987)455.
[11] JADE Coll., W. Bartel et al., Phys.Lett.**160B**(1985)421.
[12] B. Shen in ref.[2].
[13] ARGUS Coll., H. Albrecht et al., DESY 87-063, subm. to Phys.Lett.
[14] For a full discussion, see B. van Uitert, Thesis, Utrecht 1986, unpubl.
[15] Mark II Coll., G. Gidal et al., SLAC-PUB-4274 (1987).
[16] JADE Coll., W. Bartel et al., Priv. Comm.
[17] Crystal Ball Coll., D. Antreasyan et al., DESY 87-054.
[18] A. Blinov et al., Novosibirsk Preprint 87-92, 1987.
[19] TPC/2γ Coll., H. Aihara et al., Contributed Paper #297 to the Conference.
[20] PLUTO Coll., Ch. Berger et al., Phys.Lett.**149B**(1984)427;
Crystal Ball Coll., D. Antreasyan et al., Phys.Rev.**D33**(1986)1847.
[21] P. Grassberger and R. Kögerler, Nucl.Phys.**B106**(1976)451.
[22] CELLO Coll., Contributed Paper #210 to the Conference.
[23] PLUTO Coll., Ch. Berger et al., DESY 87-104, submitted to Z.Phys.C.
[24] J. Field, Proc. Intern. Europhysics Conf. on High Energy Physics, Brighton, U.K., 1983.
[25] M. Chanowitz, Proc. VIth Intern. Workshop on Photon-Photon Collisions, Lake Tahoe, California, 1984.
[26] J. Donoghue, B. Holstein and Y. Lin, Phys.Rev.Lett**55**(1985)2766; see also G. Grunberg, Phys.Lett**168B**(1986)141.
[27] F. Gilham and R. Kauffman, SLAC-PUB-4301 (1987).
[28] J. Rosner, Phys.Rev.**D27**(1983)1101.
[29] V. Druzhinin et al., Novosibirsk Preprint 87-52(1987), to be publ. in Z.Phys.C.
[30] Mark III Coll., R. Baltrusaitis et al, Phys.Rev.**D32**(1985)2883.
[31] Mark III Coll., J. Adler et al, Contributed Paper #317 to the Conference;
A. Seiden, H. Sadrozinski and H. Haber, Contributed Paper #316 to the Conference.
[32] Z. Ajaltouni et al., Contributed Paper #342 to the Conference.
[33] D. Silverman and H. Yao, Univ. of Cal. at Irvine Techn.Rep.87-3.
[34] D. Binnie et al., Phys.Lett.**83B**(1979)141.

[35] Particle Data Group, Phys.Lett.**170B**(1986)1.
[36] V. Budnev and A. Kaloshin, Phys.Lett.**86B**(1979)351.
[37] R. Graham and P. O'Donnell, Phys.Rev.**D19**(1979)284.
[38] I. Cohen and H. Lipkin, Nucl.Phys.**B151**(1979)16.
[39] S. Godfrey and N. Isgur, Phys.Rev.**D32**(1985)189.
[40] M. Frank and P. O'Donnell, Phys.Rev.**D32**(1985)1739.
[41] S. Gerasimov and A. Govorkov, Z.Phys.**C29**(1985)62; Contributed Paper #220 to the Conference.
[42] J. Prentice, Proc. Intern. Europhysics Conf. on High Energy Physics, Uppsala, Sweden, 1987.
[43] Crystal Ball Coll., pres. by H. Marsiske, Contributed Paper #88 to the Conference.
[44] Z. Ajaltouni et al., Phys.Lett.**194B**(1987)573.
[45] PLUTO Coll., CH. Berger et al., Z.Phys.**C26**(1984)199.
[46] A. Courau et al., Nucl.Phys.**B271**(1986)1.
[47] T. Barnes,K. Dooley and N. Isgur, Phys.Lett.**183B**(1987)210.
[48] D. Morgan and M. Pennington, RAL Preprint RAL-87-020 (1987); RAL Preprint RAL-87-048 (1987); Parallel Sessions, presented by M. Pennington, Proc. Intern. Europhysics Conf. on High Energy Physics, Uppsala, Sweden, 1987 (Durham Preprint DTP 87/22).
[49] R. Barbieri et al., Nucl.Phys.**B154**(1979)535; K. Hagiwara, C. Kim and T. Yoshino, Nucl.Phys.**B177**(1981)461.
[50] S. Brodsky and P. Lepage, Phys.Rev.**D24**(1981)1808;
S. Brodsky, P. Lepage and P. Mackenzie, Phys.Rev.**D28**(1983)228.
[51] M. Shifman, Z.Phys.**C4**(1980)345; Erratum Z.Phys.**C6**(1980)282.
[52] Proc. Vth Intern. Colloquium on $\gamma\gamma$ Interactions, Aachen, 1983, Springer Lecture Notes in Physics, vol. 191.
[53] J. Olsson in ref.[52]
[54] PLUTO Coll., Ch. Berger et al., Phys.Lett.**167B**(1986)120.
[55] Mark II Coll., Presented by G. Gidal, Proc. 23rd Int. Conf. on High Energy Physics, Berkeley, 1986.
[56] JADE Coll., presented by P. Hill, Proc. Intern. Europhysics Conf. on High Energy Physics, Uppsala, Sweden, 1987.
[57] TASSO Coll., U. Karshon in ref.[2].
[58] C. Baglin et al., Phys.Lett.**187B**(1987)191.
[59] A. Blinov et al., Novosibirsk Preprint 86-107, 1986.
[60] TPC/2γ Coll., H. Aihara et al., Contributed Paper #296 to the Conference.
[61] TASSO Coll., W. Braunschweig et al., Contributed Paper #351 to the Conference.
[62] D. Aston et al., Phys.Lett.**94B**(1980)113; J. Aubert et al., Nucl.Phys.**B213**(1983)31.
[63] JADE Coll., W. Bartel et al., Phys.Lett.**184B**(1987)288.
[64] S. Brodsky et al., Phys.Rev.**D19**(1979)1418; W. Stirling in ref.[52]; S. Grayson in ref.[2].
[65] TPC/2γ Coll., H. Aihara et al., Contributed Paper #306 to the Conference.
[66] TPC/2γ Coll., H. Aihara et al., Phys.Rev.Lett.**57**(1986)2500.
[67] TPC/2γ Coll., H. Aihara et al., Contributed Paper #298 to the Conference; Private Comm.
[68] Mark II Coll., G. Gidal et al., SLAC-PUB-4275 (1987).
[69] R. Cahn, Phys.Rev.**35D**(1987)3342.
[70] M. Chanowitz, Berkeley Preprint, LBL-22611, 1986, subm. for publ.
[71] V. Budnev, V. Chernyak and I. Ginzburg, Pucl.Phys.**B34**(1971)470; G. Bonneau, M. Gourdin and F. Martin, Nucl.Phys.**B54**(1973)573.
[72] V. Budnev et al., Phys.Rep.**C15**(1975)181.
[73] L. Landau, Dokl.Akad.Nauk.SSSR**60**(1948)207; C. Yang, Phys.Rev.**77**(1950)242.
[74] LASS Coll., D. Aston et al., SLAC-PUB-4340 and Nagoya Univ. preprint DPNU-87-23.
[75] K. Ispiryan and S. Matinyan, Pis'ma Zh.Eksp.Teor.Fiz.**7**(1968)232.
[76] V. Budnev, I. Ginzburg and V. Serbo, Lett. Nuovo Cimento **7**(1973)13.
[77] TASSO Coll., R. Brandelik et al., Phys.Lett.**97B**(1980)448.
[78] Mark II Coll., D. Burke et al., Phys.Lett.**103B**(1981)153; CELLO Coll., H.-J. Behrend et al., Z.Phys.**C21**(1984)205; TASSO Coll., M. Althoff et al., Z.Phys.**C16**(1982)13.
[79] PLUTO Coll., Ch. Berger et al., Contributed Paper #285 to the Conference.
[80] H. Kolanoski in ref.[52].
[81] G. Alexander, U. Maor and P. Williams, Phys.Rev.**D26**(1982)1198; G. Alexander, A. Levy and U. Maor, Z.Phys.**C30**(1986)65; A. Levy, Tel Aviv University Preprint, TAUP 1446-86, 1986
[82] N. Achasov, S. Devyanin and G. Shestakov, Phys.Lett.**108B**(1982)134; Z.Phys.**C16**(1982)55;
Pis'ma Zh.Eksp.Teor.Fiz.**40**(1984)365; Z.Phys.**C27**(1985)99.

[83] B. Li and K. Liu, Phys.Lett.**118B**(1982)435 and Erratum, Phys.Lett.**124B**(1983)550; Phys.Rev.**D28**(1983)1636; Phys.Rev.Lett.**51**(1983)1510; Phys.Rev.**D30**(1984)613.
K. Liu and B. Li, Phys.Rev.Lett.**58**(1987)2288.
[84] ARGUS Coll., H. Albrecht et al., Phys.Lett**196B**(1987)101.
[85] TPC/2γ Coll., H. Aihara et al., Contributed Paper #307 to the Conference.
[86] PLUTO Coll., Ch. Berger et al., Z. Phys.**C29**(1985)183.
[87] J. Dainton, Proc. Int. Europhysics Conf. on High Energy Physics, Brighton, U.K., 1983.
[88] N. Achasov, V. Karnakov and G. Shestakov, Novosibirsk Preprint TPh-No. 7(151), 1987.
[89] ARGUS Coll., H. Albrecht et al., DESY 87-052, to be publ. in Phys.Lett.
[90] TASSO Coll., M. Althoff et al., Z.Phys.**C32**(1986)11.
[91] TPC/2γ Coll., H. Aihara et al., Phys.Rev.Lett.**54**(1985)2564.
[92] ARGUS Coll., H. Albrecht et al., DESY 87-095, to be publ. in Phys.Lett.B
[93] S. Brodsky, G. Köpp and P. Zerwas, Phys.Rev.Lett.**58**(1987)443.
[94] H. Kolanoski, Contributed paper #303 to the Conference.
[95] F. Erné, Proc. VIth Intern. Workshop on Photon-Photon Collisions, Lake Tahoe, California, 1984.
[96] TASSO Coll., W. Braunschweig et al., Contributed Paper #327 to the Conference.
[97] E. Witten, Nucl.Phys.**B120**(1977)189; W. Bardeen and A. Buras, Phys.Rev.**D20**(1979)166; D. Duke and J. Owens, Phys.Rev.**D22**(1980)2280.
[98] PLUTO Coll., Ch. Berger et al., Phys.Lett.**107B**(1981)424; Phys.Lett.**142B**(1984)111; Nucl.Phys.**B281**(1987)365; CELLO Coll., H. Behrend et al., Phys.Lett.**118B**(1983)211; Phys.Lett.**126B**(1983)391; JADE Coll., W. Bartel et al., Phys.Lett.**121B**(1983)203; Z.Phys.**C24**(1984)231; TASSO Coll., M. Althoff et al., Z.Phys.**C31**(1986)527.
[99] TPC/2γColl., H. Aihara et al., Phys.Rev.Lett.**58**(1987)97.
[100] TPC/2γColl., H. Aihara et al., Z.Phys.**C34**(1987)1.
[101] V. Blobel, CERN School of Computing, Aiguablava, Spain (1984).
[102] TPC/2γColl., H. Aihara et al., Contributed Paper #299 to the Conference.
[103] I. Antoniadis and G. Grunberg, Nucl.Phys.**B213**(1983)445; I. Antoniadis and L. Marleau, Phys.Lett.**161B**(1985)163; Proc. 23rd Int. Conf. on High Energy Physics, Berkeley, 1986; G. Grunberg in [2].
[104] C. Petersen, T. Walsh and P. Zerwas, Nucl.Phys.**B229**(1983)301.
[105] W. Wagner, Aachen Report PITHA 83/03.
[106] A. Buras and K. Gaemers, Nucl.Phys.**B132**(1978)249.
[107] W. Wagner, Proc. 23rd Int. Conf. on High Energy Physics, Berkeley, 1986.
[108] W. Stirling, these Proceedings.
[109] C. Hill and G. Ross, Nucl.Phys.**B148**(1979)373; M. Chase, Nucl.Phys.**B189**(1981)461.
[110] W. Wagner, Proc. VIth Intern. Workshop on Photon-Photon Collisions, Lake Tahoe, California, 1984.
[111] J. Field, F. Kapusta and L. Poggioli, Phys.Lett.**181B**(1986)362; Proc. 23rd Int. Conf. on High Energy Physics, Berkeley, 1986; Z.Phys.**C36**(1987)121.
[112] M. Glück and E. Reya, Phys.Rev.**D28**(1983)2749; M. Glück, K. Grassie and E. Reya, Phys.Rev.**D30**(1984)1447.
[113] CELLO Coll., Presented by L. Poggioli, Contributed Paper #214 to the Conference.
[114] W. Frazer, Phys.Lett.**194B**(1987)287.
[115] E. Gotsman and A. Levy, Contributed Paper #219 to the Conference.

Discussion

N. Wermes (CERN): In light of the different spin-parity assignments of $\gamma\gamma \to \rho^0\rho^0$ (0^+ or 2^+) and $J/\psi \to \gamma\rho\rho$ at masses below 2 GeV, it would be interesting to compare also $J/\psi \to \gamma\omega\omega$ with the new $\gamma\gamma \to \omega\omega$ data from ARGUS. Even with the scarce data in the $\gamma\gamma$ measurement the distribution of the angle between the decay planes of the ω's should yield some information on whether 0^- or $(even)^+$ is dominant, because the expectations for these J^P's are very different.

J. Olsson: ARGUS is the only experiment so far which have observed $\gamma\gamma \to \omega\omega$ and they have only 29 events. I do not know if they looked into this problem.

A. Nilsson (McGill, ARGUS): There is not enough statistics to draw any conclusions from the distribution.

U. Maor (Tel-Aviv and DESY): Could you comment on the Q^2 dependence of $\gamma\gamma \to V_1V_2$? How does it relate to GVDM, factorization etc.?

J. Olsson: This was one of the topics for which there was no time for presentation in the talk. The measured Q^2 dependence for $\gamma\gamma \to \rho^0\rho^0$ from PLUTO and the comparison with VDM and factorization is included in the written version.